Supplementary materials

This file provides additional information on model structure, parameters, calibration and outputs, HPV vaccination and cervical screening scenarios used for health economics evaluation, and supplemental results on model simulation.

Supplement to Yuwei Li, Yi-Fan Lin, Boyu Cai, Fangfang Chen, Quanfu Zhang, Siyang Liu, Jianxin Zhen. *Modelling the epidemic dynamics of HPV among women in China and optimization of ongoing cervical cancer elimination strategies.*

Contents

1. Model structure

In this study, we developed a population-based model and an individual-based stochastic model according to the same natural history structure. The population-based model was used to fit the real-world epidemic dynamics of HPV from October 2020 to December 2023 under ongoing cervical cancer elimination strategies and calibrate the parameters. The individual-based model was used to obtain the long-term trends since 2023 and evaluate the health economics benefits of alternative interventions. Ordinary Differential Equation (ODE) and Markov Chain Monte Carlo (MCMC) were applied to the simulation of population-based and individual-based model, respectively.

1.1. Natural history

Figure S1 shows the natural history of high-risk HPV (hr-HPV) infection and related cervical carcinogenesis among females. The structure was compartmental and hybrid, consisting of a dynamic model pattern to simulate HPV transmission, and a natural history model pattern to predict cervical carcinogenesis trends. A background natural birth rate was assumed to better fit long-term epidemics. Age- and region-stratified all-cause mortality was assumed in all health states.

Susceptible-infectious-recovered-susceptible (SIRS) structure was applied to illustrate HPV transmission pattern. Neonates were assumed to be uninfected and would enter the susceptible state at their early sexually active age 14. Susceptible individuals would get infected with hr-HPV through heterosexual partnership at stratified partner acquisition rates. Those infected became immediately infectious without latent period but there was an incubation period when clinical symptom was hidden. Individuals could get rid of HPV infections and remain naturally immune until antibodies waned. 18 types of hr-HPV including HPV-16, 18, 26, 31, 33, 35, 39, 45, 51, 52, 53, 56, 58, 59, 66, 68, 73 and 82 were considered in this study, and were assumed the same transmission pathway except with genotype-specific infection and clearance rates.

The cervical carcinogenesis pattern was illustrated by precancerous stage (cervical intraepithelial neoplasia, CIN, grade 1 to 3) and cervical cancer (CC, stage I to IV). In the model, continuous infection of any-type hr-HPV may deteriorate into CIN, and genotype-specific risks of cancerization

were only determined by their clearance rates. Patients with cervical cancer were assumed to be initially asymptomatic (ACC, stage I to IV), who would enter the advanced asymptomatic state or display detectable symptoms at independent probabilities. Early, advanced and terminal cancer were subjected to different death rates. Cancer patients who remained alive for no less than 5 years moved to the survivor state and were break from subsequent simulation. Individuals in precancerous stage could clear their infection, while those progressing to cervical cancer would never naturally recover. The development and recovery procedure of CIN and CC were assumed in step-by-step manner. The staging of cervical carcinogenesis was according to the International Federation of Gynecology and Obstetrics (FIGO).

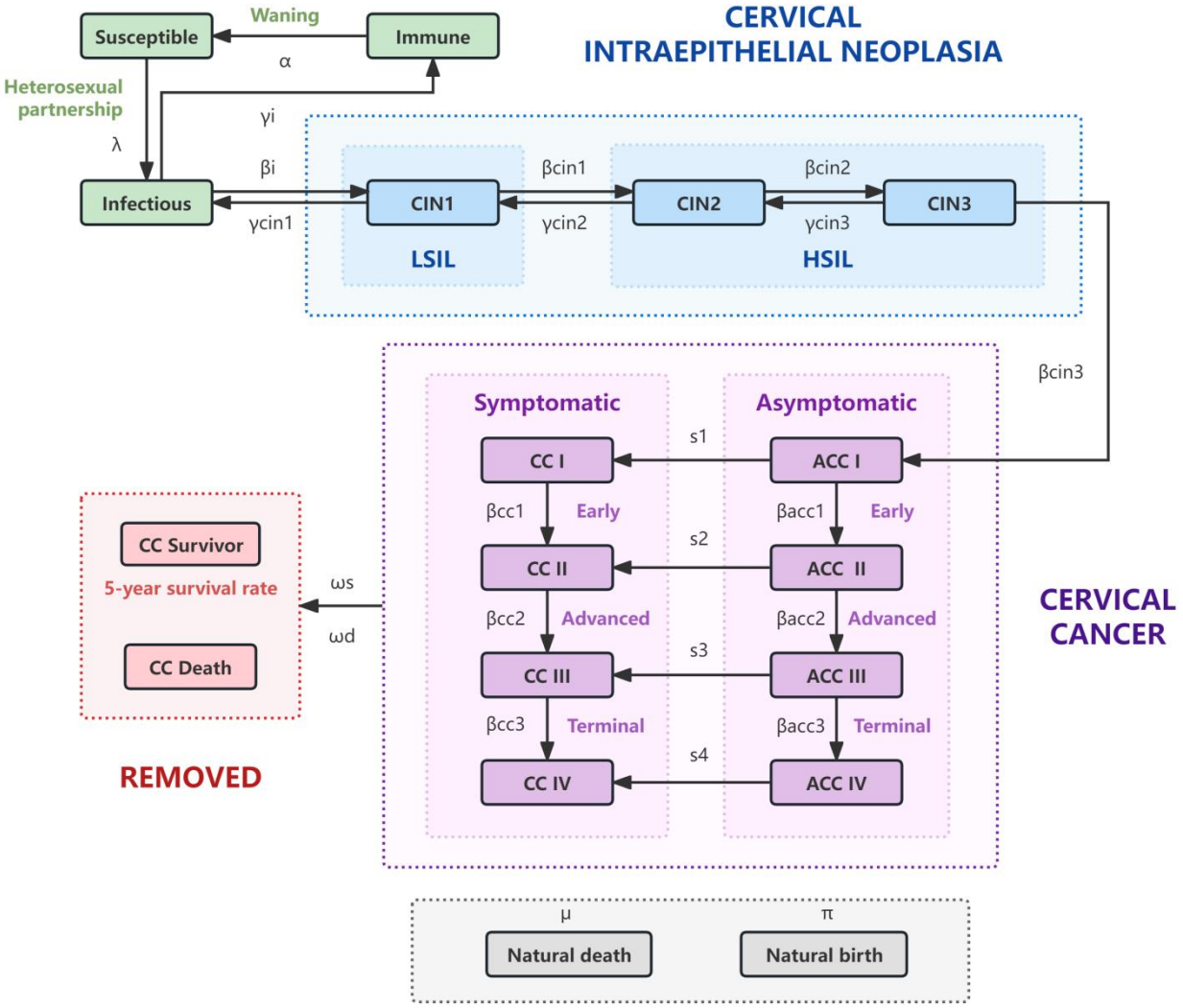

Figure S1. The natural history of HPV epidemic among females

Rectangular compartments represent health states. Lines with arrowhead represent transitions

between compartments and their directions. Early cervical cancer refers to stage I, advanced cancer refers to stage II and III, and terminal cancer refers to stage IV. Abbreviations: CIN, cervical intraepithelial neoplasia; LSIL, low-grade squamous intraepithelial lesions, including CIN1; HSIL, high-grade squamous intraepithelial lesions, including CIN2 and CIN3; ACC, asymptomatic cervical cancer; CC, symptomatic cervical cancer.

Figure S2 shows a brief natural history of hr-HPV infection and related cancerization among males. Similar SIRS and stepwise carcinogenesis structure as among females were applied. A combined state of anal, penile, and oropharyngeal cancer was established. Low-grade intraepithelial lesions was defined as the pre-stage I of either anal, penile, or oropharyngeal cancer. High-grade intraepithelial lesions was defined as the pre-stage II to III of ano-genital-oropharyngeal cancer. Individuals with any intraepithelial lesions category could clear HPV infection. Cancer patients would not recover and struggle with death. The overall transition and mortality rate of combined carcinogenesis states referred to Simons et al. Those who died of and survived for no less than 5 years from cancer were removed from model simulation.

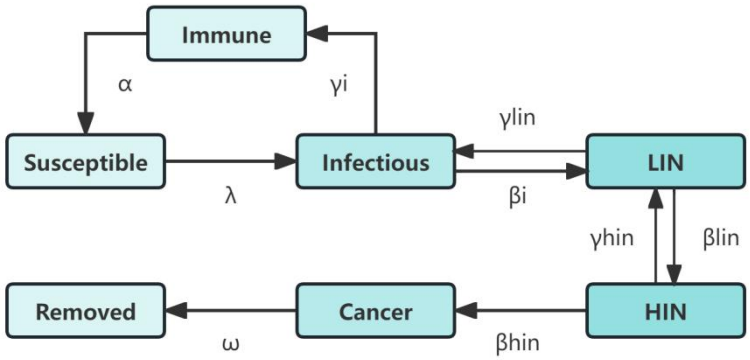

Figure S2. The natural history of HPV epidemic among males

Abbreviations: LIN, low-grade intraepithelial lesions; HIN, high-grade intraepithelial lesions.

The stratification and sexual mixing structure is shown as Figure S3. The females and males were divided into n age groups respectively (n=8; 1-14, 15-24, 25-34, 35-44, 45-54, 55-64, 65-74 and ≥75 years old), namely f1, f2,..., fn and m1, m2,..., mn. In each age group there was an additional region

stratification (urban and rural). Individuals in each subgroup were infected with hr-HPV through susceptible-infectious heterosexual contact with their partners at different ages and regions. The sexual mixing matrices depended on the partner acquisition rates and the assortativity of age and region. The force of infection (FOI, λ) was determined by the prevalence of HPV among opposite sex counterpart, the sexual mixing matrices and the transmission probability (β).

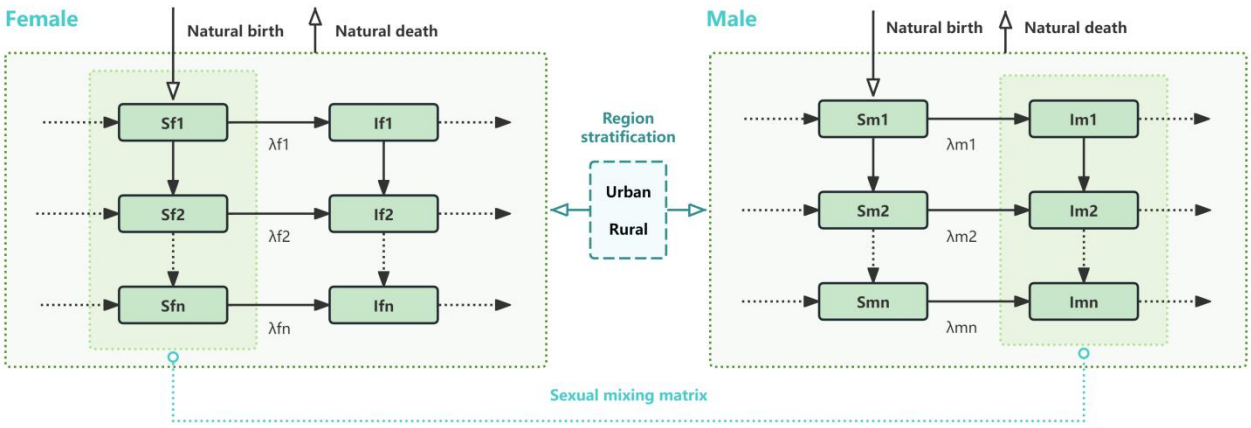

Figure S3. The stratification and sexual mixing structure

Abbreviations: S, susceptible; I, infectious. The index f and m refer to female and male, respectively; number 1 to n refer to age stratification.

1.2. Interventions

The pre-exposure prophylaxis against HPV infection considered in the model included condom use and vaccination. We assumed that the transmission probability of HPV per susceptible-infectious partnership decreased during protected intercourse. Susceptible individuals were vaccinated with either bivalent (Cecolin, Wantai Biological), quadrivalent (Gardasil, Merck) or ninvalent (Gardasil, Merck) vaccines under different rates and full adherence. Vaccinated individuals enjoyed declined FOIs of targeted HPV genotypes. We assumed that vaccine-acquired immunity was lifelong. The diagram of HPV vaccination and waning immunity was shown in Figure S4 (A).

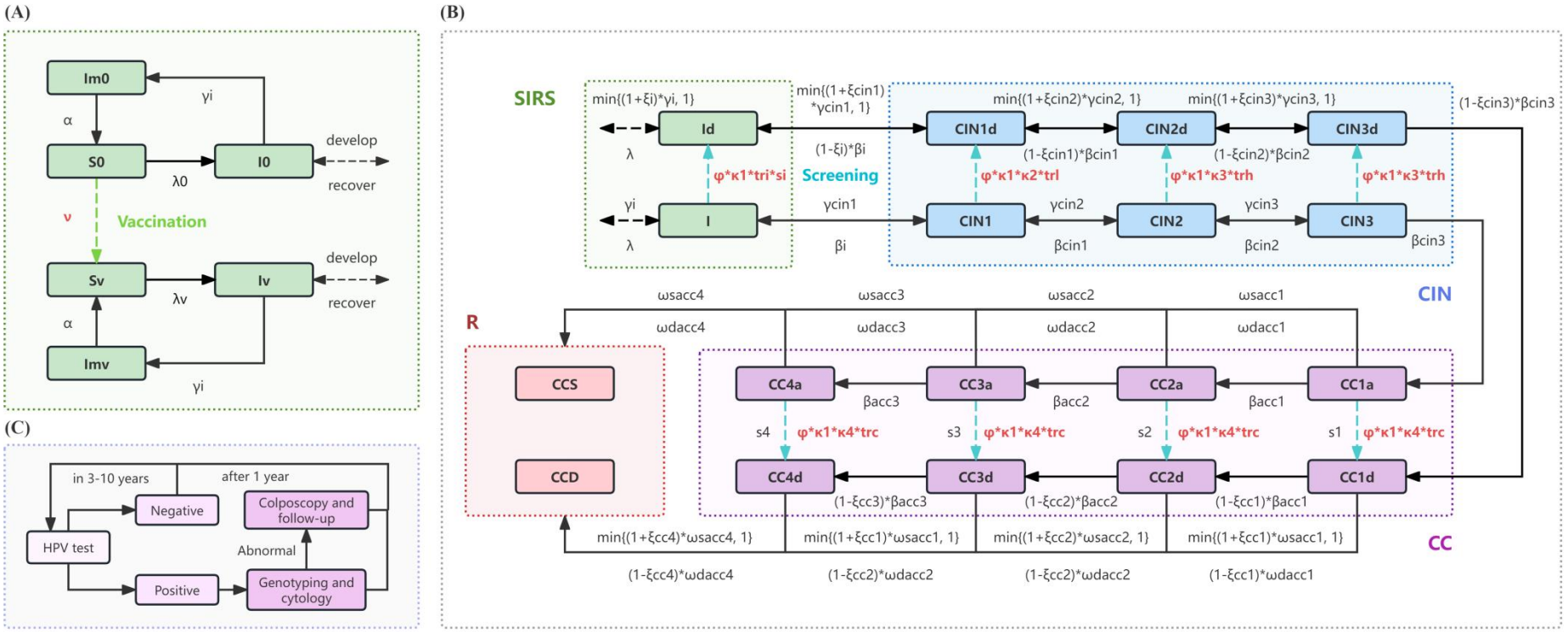

Figure S4. Model structure of preventive interventions. (A), Diagram of HPV vaccination and waning immunity. **(B)**, Diagram of cervical screening and formula of transition probabilities under treatment. **(C)**, Ongoing algorithm of regular cervical screening.

The green dashed line in (A) represents vaccination of either bivalent, quadrivalent or ninvalent HPV vaccines. The blue dashed lines in (B) represent regular cervical screening. Abbreviations: S, susceptible; I, infectious; Im, immune; CIN, cervical intraepithelial neoplasia; CC, cervical cancer; CCS, survivor from cervical cancer; CCD, death from cervical cancer. Index 0 and v refer to unvaccinated and vaccinated cohort, respectively; index a and d refer to undiagnosed asymptomatic cases and diagnosed cases, respectively. The implications and references of all parameters were shown in Chapter 2. Model inputs.

The detection and diagnosis of HPV infection and cervical cancerization was realized by cervical screening. The currently recommended cervical screening algorithm was primary HPV testing and cytology triage. As shown in Figure S4 (C), females with positive HPV testing result underwent genotyping and cytology screening, followed by colposcopy examination among those with abnormal cytology. Follow-up screening was conducted after 1 year if no lesion was detected. The regular screening program covered females aged 35-64 years and was conducted every 3-10 years, according to the World Health Organization. Self-initiated screening took place only when cancer symptoms arose (immediately diagnosed). HPV infections in incubation period would not be detected.

Diagnosed individuals would be treated at region-stratified treatment acceptance rates (tr), which were higher among those with severer neoplasia. Pure HPV infections were not provided treatment. We assumed that the risks of disease development and death among treated patients would decrease, while that of recovery and survival would increase. The declined forward and increased backward probabilities were determined by treatment efficacy (ξ). Formulas were displayed in Figure S4 (B). The treatment methods for precancerous lesions and cervical cancer included surgery, radiotherapy, and chemotherapy. Specific methods depended on the severity of cancerization condition. We assumed that cryotherapy and thermal ablation (TA) were the primary options for early precancerous lesions; photodynamic therapy including cold knife conization (CKC) and loop electrosurgical excision procedure (LEEP) was preferred for advanced lesions; hysterectomy and healthcare such as radiotherapy, chemotherapy, and home care are more necessary for cancer patients.

2. Model inputs

2.1. Force of infection

The force of infection (FOI) was defined as the risk that susceptible individuals become infected, which was given by:

$$\lambda_f(a, r, k) = \beta * \Sigma_{(i,j)} \sigma_f(a, r, i, j) * c_f(a, r) * p_m(i, j, k) \quad (2\text{-}1)$$

$$\lambda_m(i,j,k) = \beta * \Sigma_{(a,r)}\sigma_m(i,j,a,r) * c_m(i,j) * p_f(a,r,k) \quad (2\text{-}2)$$

where a and i denote the age group of females and males; r and j denote the region stratification of females and males; k denotes the HPV genotype. As HPV vaccination could effectively prevent targeted hr-HPV infection, we adjusted the genotype-specific FOIs among vaccinated population:

$$\lambda 0_f(a,r,k) = \lambda_f(a,r,k) \quad (2\text{-}3)$$

$$\lambda v_f(t,a,r,k) = [1 - VE(t,k)] * \lambda_f(a,r,k) \quad (2\text{-}4)$$

where t denotes the vaccine type. The implications of symbols were explained as follows:

Table S1. Symbol implications in FOI formula

Symbol	Implication
λ_f(a, r, k)	FOI of HPV genotype k among females in (age group a, region r)
λ_m(i, j, k)	FOI of HPV genotype k among males in (age group i, region j)
$\lambda 0_f$(a, r, k)	FOI of HPV genotype k among unvaccinated females in (age group a, region r)
λv_f(t, a, r, k)	FOI of HPV genotype k among vaccinated females in (age group a, region r) with vaccine type t
σ_f(a, r, i, j)	the probability of a female at status (a, r) whose male partner belongs to status (i, j)
σ_m(i, j, a, r)	the probability of a male at status (i, j) whose female partner belongs to status (a, r)
c_f(a, r)	the partner acquisition rate for female (a, r)
c_m(i, j)	the partner acquisition rate for male (i, j)
p_f(a, r, k)	the prevalence of HPV genotype k among females at status (a, r)
p_m(i, j, k)	the prevalence of HPV genotype k among males at status (i, j)
β	the transmission probability of HPV per susceptible-infectious partnership
VE	the genotype-specific vaccine efficacy

The initial prevalence of HPV among females in model calibration was estimated from real-world data. The prevalence of HPV among females in model simulation referred to the study by Li et al (Table S2 (a))[1]. The prevalence of HPV among males referred to a cross-sectional study by Wang et al (Table S2 (b))[2]. VE was shown in Table S9. The transmission probability β was calculated by:

$$\beta = \beta_0 * (1 - P_{condom}) + \beta_0 * (1 - E_{condom}) * P_{condom} \quad (2\text{-}5)$$

where β_0 denotes the transmission probability of HPV during unprotected intercourse (0.8232, 0.8199-0.8266); P_{condom} denotes the proportion of condom use, with a value of 0.5835[3]; E_{condom} denotes the efficacy of condom against virus transmission, ranging from 0.74 to 1[4]. The calculated β

ranged from 0.4784 to 0.5695.

Table S2 (a). Genotype-specific hr-HPV prevalence among females in China (%)

Genotype	Prevalence				
	24-	25-34	35-44	45-54	55+
16	5.48	4.49	5.6	5.26	7.56
18	1.44	1.18	1.47	1.38	1.99
26	0.04	0.03	0.05	0.04	0.05
31	0.98	0.8	1	0.94	1.35
33	1.36	1.12	1.39	1.31	1.88
35	0.4	0.32	0.4	0.38	0.55
39	1.17	0.96	1.19	1.12	1.61
45	0.32	0.26	0.33	0.31	0.44
51	1	0.82	1.02	0.96	1.37
52	3.49	2.86	3.56	3.35	4.81
53	1.46	1.20	1.49	1.40	2.01
56	0.36	0.29	0.37	0.34	0.49
58	1.47	1.2	1.5	1.41	2.03
59	0.69	0.56	0.7	0.66	0.95
66	0.86	0.7	0.88	0.83	1.19
68	1.09	0.89	1.12	1.05	1.51
73	0.0001	0.0001	0.0001	0.0001	0.0001
82	0.2	0.17	0.21	0.19	0.28

Table S2 (b). Genotype-specific hr-HPV prevalence among males in China (%)

Genotype	Prevalence				
	24-	25-34	35-44	45-54	55+
16	10.75	8.65	8.5	8.05	8.62
18	4.1	3.3	3.96	3.3	2.33
26	0.0001	0.0001	0.0001	0.0001	0.0001
31	1.76	1.41	1.7	1.41	1
33	0.97	0.78	0.94	0.78	0.55
35	0.97	0.78	0.94	0.78	0.55
39	3.32	2.67	3.21	2.67	1.88
45	0.59	0.47	0.57	0.47	0.33
51	2.93	2.36	2.84	2.36	1.67
52	3.13	2.52	3.02	2.52	1.77
53	2.54	2.04	2.45	2.04	1.44
56	1.76	1.41	1.7	1.41	1

58	6.46	5.2	6.24	5.2	3.67
59	1.56	1.26	1.51	1.26	0.89
66	2.34	1.89	2.27	1.89	1.33
68	1.76	1.41	1.7	1.41	1
73	0.4	0.32	0.38	0.32	0.23
82	0.4	0.32	0.38	0.32	0.23

2.2. Sexual mixing

As described by Barnabas et al, we calculated the assortativity of age and region as follows[5]:

$$\sigma_f(a,r,i,j) = \left\{\varepsilon_1 * \frac{\sum_j n_m(i,j) * c_m(i,j)}{\sum_{(i,j)} n_m(i,j) * c_m(i,j)} + (1-\varepsilon_1) * \delta(a,i)\right\} * \left\{\varepsilon_2 * \frac{n_m(i,j) * c_m(i,j)}{\sum_j n_m(i,j) * c_m(i,j)} + (1-\varepsilon_2) * \delta(r,j)\right\} \quad (2\text{-}6)$$

$$\sigma_m(i,j,a,r) = \left\{\varepsilon_1 * \frac{\sum_r n_f(a,r) * c_f(a,r)}{\sum_{(a,r)} n_m(i,j) * c_m(i,j)} + (1-\varepsilon_1) * \delta(i,a)\right\} * \left\{\varepsilon_2 * \frac{n_f(a,r) * c_f(a,r)}{\sum_r n_f(a,r) * c_f(a,r)} + (1-\varepsilon_2) * \delta(j,r)\right\} \quad (2\text{-}7)$$

where $n_m(i, j)$ denotes the number of male (i, j); $n_f(a, r)$ denotes the number of female (a, r). ε is the mixing coefficient (0=assortative, 1=random); ε_1 denotes the mixing coefficient by age (0.9); ε_2 denotes the mixing coefficient by region (0.8). δ is the identity matrix (1 if i=k, 0 otherwise).

The partner acquisition rates were estimated based on the sexual intercourse frequency among fixed partners (Table S3), the proportion of no sexual partners, fixed partners, and multiple partners referred to the Family Planning Association of Hong Kong[6], as well as the average number of multiple partners (2.5/6 months[7]), according to formulas (2-8) and (2-9).

$$c_f(a,r) = 0 * sp_{0_f}(a,r) + c_{1_f}(a,r) * sp_{1_f}(a,r) + n_{sp} * sp_{n_f}(a,r) \quad (2\text{-}8)$$

$$c_m(i,j) = 0 * sp_{0_m}(i,j) + c_{1_m}(i,j) * sp_{1_m}(i,j) + n_{sp} * sp_{n_m}(i,j) \quad (2\text{-}9)$$

where sp_0, sp_1 and sp_n denote the proportion of individuals with no sexual partner, fixed sexual partner, and multiple sexual partners, respectively. c_1 denotes the sexual intercourse frequency among fixed partners, and n_{sp} denotes the average number of multiple partners.

Table S3 (a). Stratified sexual intercourse frequency (per month) for females in China[8-10]

	Region		
Age	overall	urban	rural
24-	1.50	1.10	2.23
25-44	5.70	4.17	8.51
45-54	3.88	2.84	5.79
55+	0.17	0.12	0.25

Table S3 (b). Stratified sexual intercourse frequency (per month) for males in China[8-11]

	Region		
Age	overall	urban	rural
24-	1.67	1.03	2.85
25-44	6.80	4.18	11.60
45-54	4.31	2.65	7.36
55+	0.17	0.10	0.29

2.3. Demographic data

We extracted demographic data from China Health Statistics Yearbook, National Bureau of Statistics of China and open-source publications (Table S4-S6)[12]. The nationwide population size was 689.49 million females and 723.11 million males; that in Shenzhen was 7.89 and 9.67 millions of females and males, respectively, according to Shenzhen Municipal Bureau of Statistics[13]. The within-group ages were assumed to be uniformly distributed. The initial distribution of health states in model fitting was estimated with real-world epidemiological data.

Table S4. Population structure

Age	**Female**		**Male**	
	urban	rural	urban	rural
14-	10.88%	5.93%	11.73%	6.40%
15-24	6.47%	3.53%	7.10%	3.87%
25-34	9.35%	5.10%	9.68%	5.28%
35-44	8.94%	4.87%	9.01%	4.91%
45-54	10.66%	5.81%	10.47%	5.71%
55-64	8.53%	4.65%	8.19%	4.46%
65-74	6.24%	3.40%	5.68%	3.10%
75+	3.65%	1.99%	2.85%	1.55%

Table S5. Natural birth rate (per 1000 persons)

Gender	Region	
	urban	rural
female	2.38	1.29
male	2.49	1.36

Table S6. Age-standardized natural death rate (per 100000 persons)

Age	Female		Male	
	urban	rural	urban	rural
neonate	176.42	207.22	155.33	181.07
14-	15.56	22.20	12.82	16.56
15-24	33.06	42.93	18.19	21.27
25-34	50.42	86.16	21.51	33.22
35-44	124.65	178.68	48.50	65.47
45-54	310.57	425.65	128.54	175.11
55-64	779.32	959.42	315.19	428.63
65-74	2073.47	2313.43	1042.10	1296.15
75+	7663.24	8681.64	6288.83	6939.90

NOTE: Age-standardized rate was defined as the weighted average of rates in age groups with smaller age difference. For example, $d_{15\text{-}24}=p_{15\text{-}19}*d_{15\text{-}19}+p_{20\text{-}24}*d_{20\text{-}24}$, where d denotes the within-group death rate and p denotes constituent ratio.

2.4. Transition parameters

The transition parameters in the model were derived from published literature, including mathematical modelling, clinical trials and observational cohort studies. The details were summarized in Table S7. Table S8 shows the stratified hr-HPV clearances. The transition from infectious to immune was assumed with HPV genotype-specific rate, which was calculated as the clearance divided by the infection duration. In consideration of the heterogeneity among studies, all parameters were supposed to be uniformly distributed within a wide range. In the population-based model simulation under ongoing preventive strategies, we calculated the quarterly rates as the annual rates divided by 4.

The uncalibrated parameters were components of the state transition equations. For instance, assuming that the total number of females in susceptible, infectious, immune, and CIN1 states at time

t are S_f (t), I_f(t), Im_f (t), and CIN1 (t), respectively, and at each time interval:

- Susceptible individuals have a probability of being infected with FOI=λ_f ;
- Infected individuals clear hr-HPV infection with a probability of γ_{if} and develop CIN1 with a probability of β_{if};
- Individuals who have cleared hr-HPV infection and obtained natural immunity recover to susceptibility at an average of $1/\alpha_f$ time intervals;
- CIN1 patients recover to infected state with a probability of γ_{cin1};
- The natural birth rate among the population is π_{bf}, the natural mortality rate is π_{df}, the age growth rate is μ_f, and a, r, and k are age, region, and genotype stratification, respectively. Therefore, the ODE is constructed as follows:

$$dS_f(a,r) = -\sum_k \lambda_f(a,r,k) * S_f(a,r) + \alpha_f * Im_f(a,r) + I\{a=1\} * \sum_a \pi_{bf}(a,r) * N_f(a,r) - [\pi_{df}(a,r) + \mu_f(a)] * S_f(a,r) \quad (2\text{-}10)$$

$$dI_f(a,r,k) = \lambda_f(a,r,k) * S_f(a,r) + \gamma_{cin1} * CIN1(a,r,k) - [\gamma_{if}(a,r,k) + \beta_{if}(a,r,k) + \pi_{df}(a,r) + \mu_f(a)] * I_f(a,r,k) \quad (2\text{-}11)$$

$$dIm_f(a,r) = \sum_k \gamma_{if}(a,r,k) * I_f(a,r,k) - [\alpha_f + \pi_{df}(a,r) + \mu_f(a)] * Im_f(a,r) \quad (2\text{-}12)$$

Table S7 (a). Annual transition rates among females

Symbol	Implication	Value	Range	Source
αf	the rate of waning innate immunity	0.021	0.015-0.027	[14]
Backward rate				
γcin1	the backward transition rate from CIN1 to I	0.5044	0.4732-0.5561	[15]
γcin2	the backward transition rate from CIN2 to CIN1	0.2494	0.1994-0.2992	[15]
γcin3	the backward transition rate from CIN3 to CIN2	0.0135	0.0101-0.0169	[16,17]
Forward rate				
βif	the forward transition rate from I to CIN1	0.0450	0.0279-0.0661	[15]
βcin1	the forward transition rate from CIN1 to CIN2	0.2240	0.1608-0.2972	[16,17]

βcin2	the forward transition rate from CIN2 to CIN3	0.3498	0.2623-0.4372	[16,17]
βcin3	the forward transition rate from CIN3 to ACC1	0.1019	0.0764-0.1274	[16,17]
βacc1	the forward transition rate from ACC1 to ACC2	0.4377	0.3283-0.5471	[18,19]
βacc2	the forward transition rate from ACC2 to ACC3	0.5358	0.4019-0.6698	[18,19]
βacc3	the forward transition rate from ACC3 to ACC4	0.6838	0.5129-0.8548	[18,19]
s1	symptom development rate from ACC1 to CC1	0.15	0.11-0.19	[18]
s2	symptom development rate from ACC2 to CC2	0.23	0.17-0.29	[18]
s3	symptom development rate from ACC3 to CC3	0.60	0.45-0.75	[18]
s4	symptom development rate from ACC4 to CC4	0.90	0.68-1.00	[18]
Death rate				
ωdacc1	the death rate of ACC1	0.024	0.012-0.036	[20]
ωdacc2	the death rate of ACC2	0.044	0.024-0.064	[20]
ωdacc3	the death rate of ACC3	0.127	0.064-0.191	[20]
ωdacc4	the death rate of ACC4	0.300	0.191-0.450	[20]
Survival rate				
ωsacc1	the 5-year survival rate of ACC1	0.90	0.82-0.94	[20,21]; calculated
ωsacc2	the 5-year survival rate of ACC2	0.78	0.68-0.88	[20,21]; calculated
ωsacc3	the 5-year survival rate of ACC3	0.37	0.05-0.68	[20,21]; calculated
ωsacc4	the 5-year survival rate of ACC4	0.03	0.00-0.05	[20,21]; calculated
/	age-stratification: 44-	1.05 times of ωsacc	1.05 times of ωsacc	[21]
	45-54	1.03 times of ωsacc	1.03 times of ωsacc	[21]
	55-64	0.99 times of ωsacc	0.99 times of ωsacc	[21]
	65-74	0.92 times of ωsacc	0.92 times of ωsacc	[21]
	75+	0.76 times of ωsacc	0.76 times of ωsacc	[21]
Duration				
/	the infection duration	2 years	1-3 years	assumed

NOTE: I, infectious; CIN, cervical intraepithelial neoplasia; ACC, asymptomatic cervical cancer (undiagnosed); CC, cervical cancer (diagnosed).

Table S7 (b). Annual transition rates among males

Symbol	Implication	Value	Range	Source
αm	the rate of waning innate immunity	0.021	0.015-0.027	[14]
βim	the forward transition rate from I to LIN	0.0480	0.036-0.060	[22]
βlin	the forward transition rate from LIN to HIN	0.0052	0.0039-0.0065	[22]
βhin	the forward transition rate from HIN to invasive cancer	0.0000732	0.0000637-0.0000772	[23,24]
γim	HPV clearance rate			
	HPV16	0.38	0.285-0.475	[25]
	HPV18	0.72	0.540-0.900	[25]
	other hr-HPV	0.69	0.518-0.863	[25]
γlin	the backward transition rate from LIN to I	0.0533	0.0400-0.0666	[22]
γhin	the backward transition rate from HIN to LIN	0.0533	0.0400-0.0666	[22]
ωdc	the overall death rate of C	0.210	0.106-0.314	[24]
ωsc	the overall 5-year survival rate of C	0.692	0.629-0.755	[22]

NOTE: I, infectious; LIN, low-grade intraepithelial neoplasia; HIN, high-grade intraepithelial neoplasia; C, cancer.

Table S8. Stratified hr-HPV clearance among females in China (%)[18,26,27]

Genotype	Clearance				
	24-	25-34	35-44	45-54	55+
16	100.00, 99.91-100.00	88.50, 86.50-90.43	85.63, 83.70-87.50	71.38, 69.77-72.94	50.29, 49.16-51.39
18	99.62, 95.39-100.00	86.25, 82.59-89.73	83.46, 79.91-86.83	69.57, 66.61-72.38	49.02, 46.94-51.00
26	100, 97.5-100.00	86.95, 84.78-89.12	84.13, 82.03-86.23	70.13, 68.38-71.88	49.41, 48.17-50.65
31	95.96, 89.92-100.00	83.08, 77.86-88.00	80.39, 75.33-85.15	67.01, 62.80-70.98	47.22, 44.25-50.01
33	97.53, 92.61-100.00	84.44, 80.19-88.49	81.70, 77.59-85.62	68.11, 64.68-71.37	47.99, 45.57-50.29
35	100.00, 100.00-100.00	100.00, 94.44-100.00	100.00, 91.38-100.00	83.38, 76.18-88.81	58.75, 53.67-62.57
39	95.11, 90.64-99.40	82.35, 78.48-86.06	79.68, 75.94-83.27	66.42, 63.30-69.41	46.80, 44.60-48.91
45	100.00, 100.00-100.00	98.97, 91.62-100.00	95.67, 88.65-100.00	79.75, 73.90-84.64	56.19, 52.07-59.64
51	100.00, 100.00-100.00	90.90, 86.86-94.67	87.96, 84.05-91.60	73.32, 70.06-76.36	51.66, 49.37-53.80
52	80.00, 77.59-82.39	69.27, 67.18-71.33	67.02, 65.00-69.02	55.87, 54.18-57.54	39.37, 38.18-40.54
53	85.29, 83.16-87.42	73.84, 71.80-75.69	71.45, 69.66-77.34	59.56, 58.07-61.05	41.97, 40.92-43.02
56	100.00, 95.78-100.00	88.35, 82.92-93.37	85.49, 80.24-90.35	71.26, 66.89-75.31	50.21, 47.13-53.07
58	82.13, 78.91-85.32	71.11, 68.32-73.87	68.80, 66.11-71.48	57.35, 55.11-59.58	40.41, 38.83-41.98
59	100.00, 100.00-100.00	95.26, 89.69-100.00	92.17, 86.78-96.97	76.84, 72.34-80.84	54.14, 50.97-56.96
66	100, 97.5-100.00	86.95, 84.78-89.12	84.13, 82.03-86.23	70.13, 68.38-71.88	49.41, 48.17-50.65
68	93.83, 89.13-98.37	81.24, 77.17-85.17	78.61, 74.67-82.41	65.53, 62.25-68.70	46.17, 43.86-48.40
73	100.00, 100.00-100.00	100.00, 97.50-100.00	100.00, 94.12-100.00	85.88, 78.47-91.47	60.51, 55.28-64.45
82	100, 97.5-100.00	86.95, 84.78-89.12	84.13, 82.03-86.23	70.13, 68.38-71.88	49.41, 48.17-50.65

NOTE: The genotype-specific HPV clearance in age group i was estimated as: (Overall genotype-specific clearance)*[(Proportion of age group i among individuals getting rid of HPV infection)/(Proportion of age group i among infected individuals).

hr-HPV, high-risk HPV; 2v, bivalent vaccine preventable; 4v, quadrivalent vaccine preventable; 9v, ninvalent vaccine preventable.

2.5. Intervention parameters

Table S9 shows the coverages (a) and efficacy (b) of HPV vaccination. Referring to China Surveillance System of Information on National Immunization Program, we assumed that females aged 9-45 years were provided either bivalent, quadrivalent or ninvalent vaccine at the annual rate of 0.44% (0.33-0.55%), 1.06% (0.80-1.33%) and 0.75% (0.56-0.94%), separately in the population-based model[28]. The bivalent and quadrivalent vaccine decrease the infection risk of HPV 16 and 18; the ninvalent vaccine additionally targets at HPV 31, 33, 45, 52 and 58.

Table S9 (a). The vaccination coverages of bivalent, quadrivalent and ninvalent HPV vaccines among females aged 9-45 years in 2020[29]

Type	Region	
	urban	rural
bivalent	4.56%	3.24%
quadrivalent	10.94%	7.80%
ninvalent	7.75%	5.52%
overall	23.24%	16.55%

NOTE: The vaccination coverage was assumed to increase proportionally, which in year n was calculated as VCni=VCi*(1+υ)^(n-2020).

Table S9 (b). The efficacy of bivalent, quadrivalent and ninvalent HPV vaccines against hr-HPV infection

Symbol	Implication	Value	Range	Source
VE1	the efficacy of bivalent vaccine	94.00%	80.00–99.00%	[20,30]
VE2	the efficacy of quadrivalent vaccine	94.50%	65.20-99.90%	[25,30]
VE3	the efficacy of ninvalent vaccine	96.70%	80.90-99.80%	[31]

NOTE: hr-HPV, high-risk HPV.

Table S10 shows the stratified participation of cervical screening (a) and the sensitivities of cervical screening techniques. The result from pathological examination was regarded as the golden standard. Age-stratified screening participation rates used in model calibration were estimated from literature and real-world data, which was calculated as follows:

- Obtain the overall cervical screening participation rates among the total female population in 2020-2023 by linear regression using data from Zhang et al[32];

- Divide the screening records in Shenzhen Baoan Women's and Children's Hospital from October 2020 into 13 quarters.
- For each quarter, derive age stratification among cervical screening participants, and multiply the age composition by the corresponding overall participation in step 1.
- Derive region stratification (urban:rural=8.98:1) according to the epidemiological investigations by Mu et al[33];
- Calculate the median and interquartile range (IQR) of stratified participation rates from 13 quarters.
- The participation in group (i, j) were estimated as [Count of screening in group (i, j)/Total population]/[group (i, j)/Total population]=[Stratified screening participation rates among the total population]/[population proportion].

In model simulation, as it is known that the overall participation rate of cervical screening for women aged 35-64 in 2023 is only 36.8%[34]. The screening participation rates were adjusted according to the age and urban-rural ratio calculated above and the population composition in China.

Table S10 (a). Cervical screening participation (≥1 time) among stratified females (%)

Age	Region	
	urban	rural
14-	0.00, 0.00-0.00	0.00, 0.00-0.00
15-24	0.36, 0.18-1.03	0.08, 0.04-0.22
25-34	100.00, 100.00-100.00	58.11, 38.55-73.98
35-44	100.00, 100.00-100.00	66.04, 63.84-100.00
45-54	81.37, 76.63-100.00	16.99, 16.00-25.33
55-64	30.17, 19.65-61.25	6.30, 4.10-12.79
65-74	0.00, 0.00-0.26	0.00, 0.00-0.06
75+	0.00, 0.00-0.00	0.00, 0.00-0.00

NOTE: The participation in group (i, j) was denoted as φ(i, j), i=1, 2, ..., 8; j=1, 2 in formula.

Table S10 (b). Sensitivities of cervical screening techniques

Symbol	Implication	Value	Range	Source
κVIA	the sensitivity of VIA	0.58	0.45-0.72	[18]
κ1				
HC-2	the sensitivity of HPV testing (HC-2)	0.91	0.79-1.00	[35]
PCR	the sensitivity of HPV testing (PCR)	0.96	0.93-1.00	[36]
κ2	the sensitivity of LBC to detect LSIL	0.70	0.53-0.88	[37]

κ3	the sensitivity of LBC to detect HSIL	0.81	0.78–0.84	[37]
κ4	the sensitivity of LBC to detect cell carcinoma	0.94	0.90-0.99	[18]

NOTE: VIA, visual inspection with acetic acid; HC2, Hybrid Capture-2; LBC, liquid-based cytology; LSIL, low-grade squamous intraepithelial lesion, including CIN1; HSIL, high-grade squamous intraepithelial lesion, including CIN2, CIN3.

Table S11 shows the efficacy of cervical cancer treatment (a) and the eligibility of cryotherapy and thermal ablation in precancerous stage (b). We assumed that the base-case efficacy of hysterectomy against cervical cancer was 100%. Precancerous patients who were eligible for and accepted treatment chose specific ablative methods based on the ratio of eligibilities. Random sampling was implemented to simulate the method selection process (Figure S5).

Table S11 (a). The efficacy of treatment for cervical cancer prevention

Treatment	Value	Range	Source
Ablative treatment			
cryotherapy			
CIN	0.83	0.74–0.92	[38]
TA			
HPV infection	0.80	0.73-0.86	[39]
CIN1	0.90	0.81-0.96	[39]
CIN2/3	0.76	0.62-0.87	[39]
PDT			
CKC	0.89	0.87-0.92	[40]
LEEP	0.92	0.85–0.99	[41]
Hysterectomy	1.00	0.95-1.00	assumed

NOTE: TA, thermal ablation; PDT, photodynamic therapy; CKC, Cold knife conization; LEEP, loop electrosurgical excision procedure.

Table S11 (b). The eligibility of cryotherapy and TA[42]

Treatment	Value	Range
Cryotherapy		
CIN1	0.80	0.50-1.00
CIN2	0.70	0.50-1.00
CIN3	0.40	0.00-0.50
TA		
CIN1	0.51	0.38-0.64
CIN2	0.53	0.40-0.67
CIN3	0.45	0.34-0.56

NOTE: TA, thermal ablation.

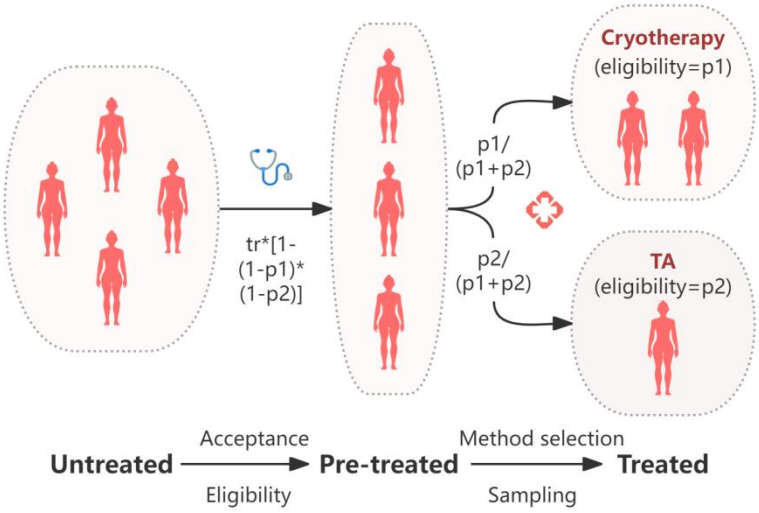

Figure S5. The flowchart of precancerous patients accepting and selecting treatment

Female patterns in red represents precancerous patients. The acceptance is denoted by tr and the eligibility is denoted by p=1-(1-p1)(1-p2), from the untreated stage to the pre-treated stage. From the pre-treated stage to the treated stage, assuming that the probability of choosing two methods is proportional to the ratio of p1 and p2, and the number of times choosing cryotherapy satisfies a Bernoulli distribution with a probability of p1/(p1+p2).*

3. Model calibration

Model calibration was implemented by determining the best-fitting parameters to the real-world HPV prevalences. The real-world trends were calculated from screening data. We collected the cervical screening records in Shenzhen Baoan Women's and Children's Hospital and divided them into quarterly subsets. As there exists data missing due to the replacement of archive system, we selected the time interval from July 2020 to December 2023 with relatively complete backup to estimate real-world HPV prevalences. The simulated trends were acquired using population-based model. We generated 10,000 combinations of parameters by performing Latin hypercube sampling, and obtained the HPV epidemic dynamics under each combination. The top 1% best-fitting parameter combinations were obtained by minimize the inverse-variance weighted mean square error (MSE) between simulated and real-world trends with age and HPV genotype stratification. The fitted

curve and its 95% confidence interval (CI) were drawn using Bootstrap method (sampling with replacement for 50 times; repeat for 1,000 rounds). The overall determination coefficient (R^2) was calculated to evaluate the calibration effect.

3.1. Real-world epidemiological data

A total of 132,282 records were retained after deleting repeated measurement data. All records were divided into 14 subsets by quarter from July 2020, namely 2020Q3, 2020Q4, 2021Q1, ..., 2023Q4. Records in 2020Q3 was used to calculated the initial state of model simulation. The records include the results from HPV nucleic acid test, HPV genotyping, thin-layer cytology test (TCT) and pathology test. In each quarterly subset, we merged the four categories of test results according to the patient ID, retained the last record of the same ID, and randomly sampled into the training set and the testing set (6:4) according to the principle of equal age distribution. The training set was used for model parameter fitting and optimization, while the testing set was used to evaluate the calibrated model and internally validated the model accuracy in predicting the trend of hr-HPV. During partitioning, Kolmogorov Smirnov, Wilcoxon, and Friedman non-parametric tests were used to ensure that the real-world prevalence distributions calculated by the two were consistent. The significance level of the test is set at 0.05. Subsequently, the number of screening participants (sample size), and hr-HPV overall, age-stratified, and genotype-specific prevalences were calculated for each quarter on both the two sets. As there are cases failed to be followed up between screening steps, the prevalence of HPV was calculated by the product of conditional probabilities, that is:

$$Genotype-specific\ prevalence\ =\ (HPV\ positive\ rate\ in\ HPV\ nucleic\ acid\ test)\ *\ (Proportion\ of\ genotype\ in\ HPV\ genotyping) \quad (3\text{-}1)$$

and the precancerous and cancer prevalences were calculated as the proportion of confirmed abnormal results in either TCT or pathology test, to the total number of screening participants.

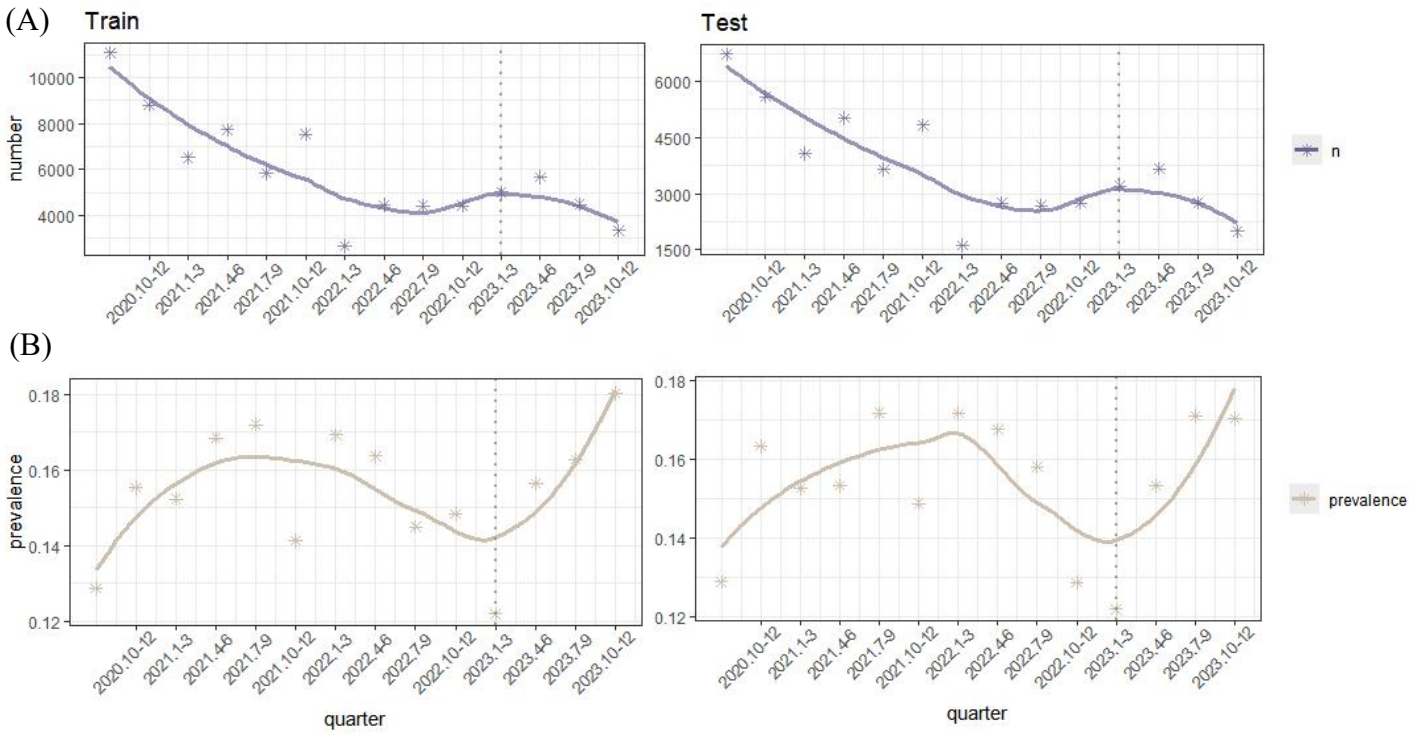

Figure S6. The quarterly number of screening participants and HPV prevalence, calculated by screening records. (A) The total number of screening records, merged by patient id. (B) The overall real-world HPV prevalence.

The curves were fitted by spline interpolation. The points in hollow circle represent the exact values. ntest, the number of participants attending HPV testing; prevalence, the prevalence of HPV.

3.2. Parameter fitting

We randomly divided the dataset into a training set for parameter fitting and a testing set for the internal validation of calibrated model, with the ratio of 6:4. The algorithms for HPV prevalence were the same for both of the subsets. We conducted model fitting based on several considerations:

- The entire time interval covers the period of COVID-19 endemic, during which lockdown and lower screening participation were observed (Figure S6). A segmented model consisting of a during-covid and a post-covid component was therefore constructed regarding 2022Q4 as the breakpoint. Two additional parameters cd and sd, which denote the decrease in contact and screening rate respectively, were assumed with range 0-1 to join in the calibration of during-covid model. (Figure S7)

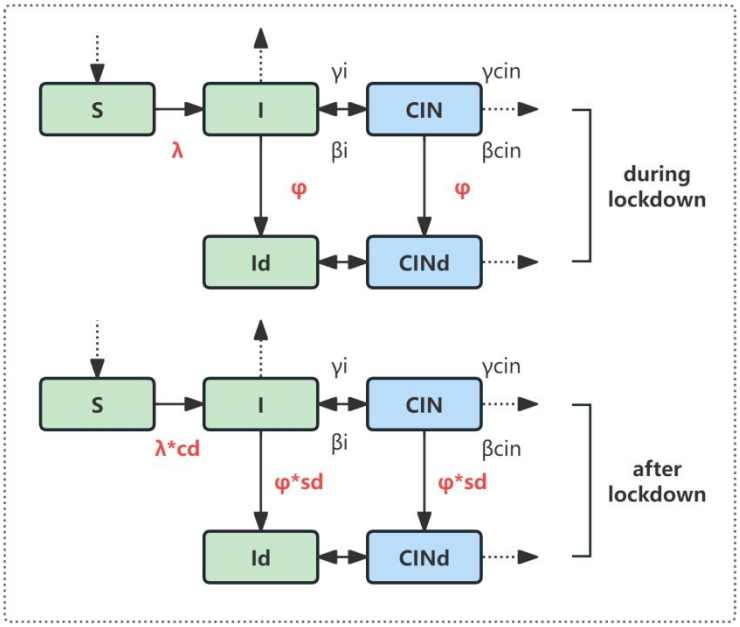

Figure S7. The segmented model structure according to COVID-19 lockdown status

λ: the force of transmission; φ: the screening participation rate.

- The age distribution of screening participants was different from that in model simulation. We extracted the quarterly age distribution ratio of real-world dataset. The overall simulated prevalence curve was adjusted to be with the same age structure.
- The inaccuracy of cervical screening led to bias in HPV diagnosis. We adjusted the real-world value (p) by:

$$p0 = p * sensitivity + (1 - p) * (1 - specificity) \quad (3\text{-}2)$$

$$i.e.\ p = (p0 - 1 + specificity)/(sensitivity - 1 + specificity) \quad (3\text{-}3)$$

where p0 denotes the originally calculated prevalence from screening records.

Figure S8 presents the fitting effect after calibration on the testing set. The fitting R^2 of overall HPV prevalence reached 0.71.

(A)

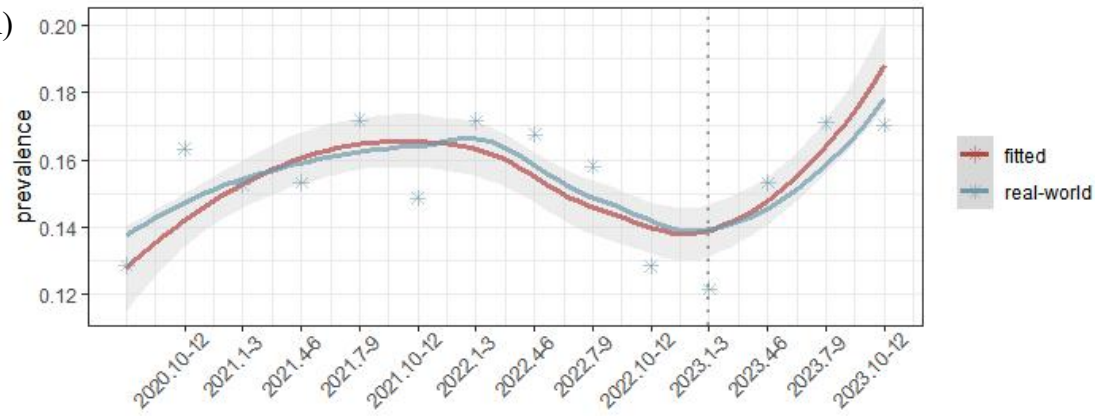

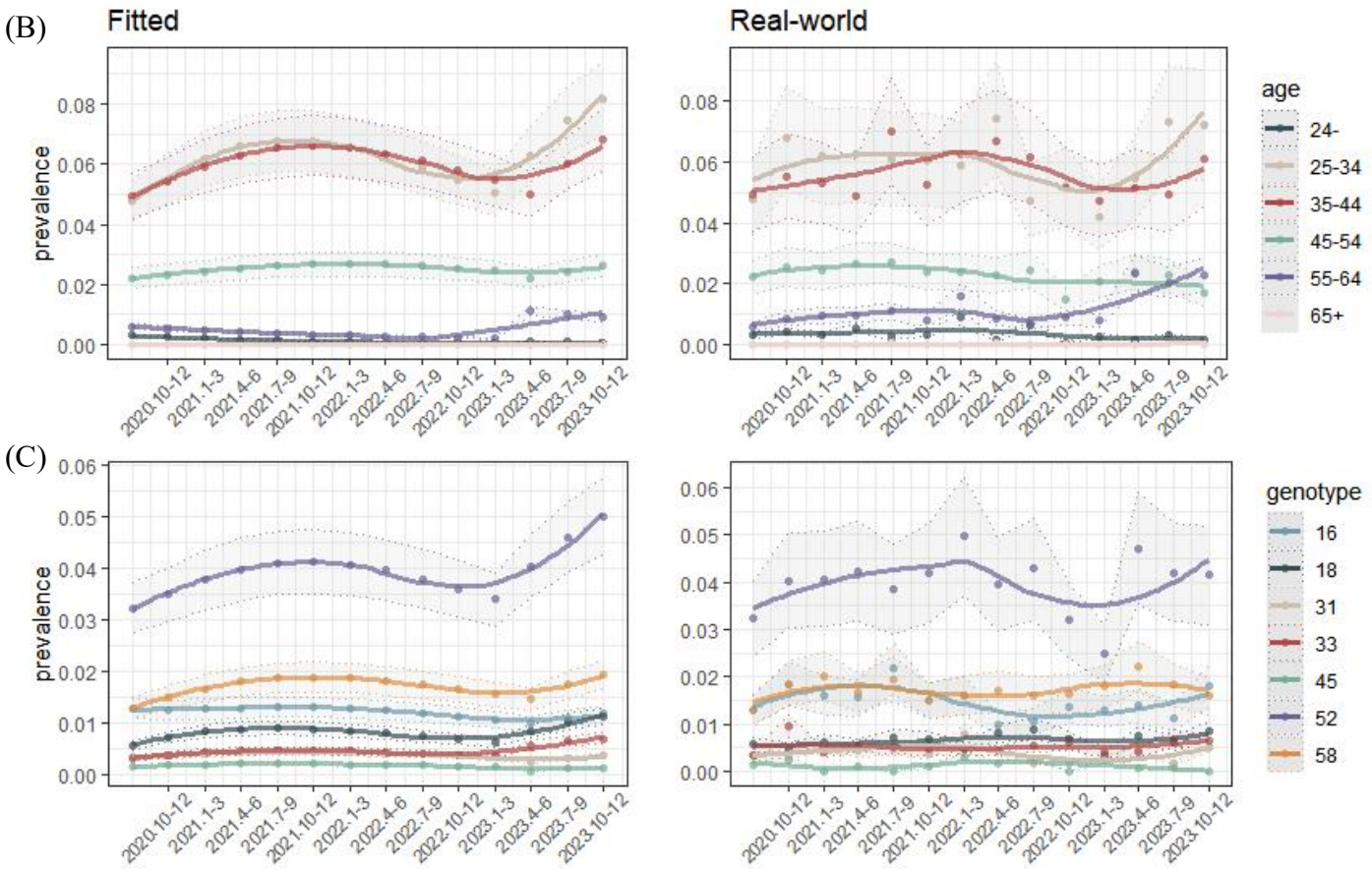

Figure S8. The real-world and fitted curves of HPV prevalence. (A) The overall HPV prevalence. (B) The age-stratified prevalences. (C) The genotype-specific prevalences of 9v-HPV.

The blue vertical dashed line in (A) represents the breakpoint of modelling. For (B) and (C), the figure on the left represents the fitted curve; that on the right represents the real-world curve. Number 1-13 in x-axis denote the quarters 2020Q4, 2021Q1, ..., 2023Q4, respectively.

4. Model simulation

In this study, the population-based model was used to simulate the epidemic trends of hr-HPV infections and cervical cancers within 10 years under ongoing strategies, while observing the short-term effects of adjusting intervention parameters under the current distribution of health status among females, as well as providing optimization directions for the ongoing strategies. The individual-based model was used to simulate the long-term effects of different intervention scenarios among females initially before sexual activity, and select the optimal intervention scenario. The

population-based model was simulated among the total female population, and the initial health status distribution was calculated based on the epidemiological data in 2023; the individual-based model was simulated among a 75-year intervention cohort of 100,000 females, who were initially completely susceptible and whose initial age followed a uniform distribution under 14 years old. When evaluating the intervention effect, the baseline scenario was set as no HPV vaccination or cervical screening, and the model was run for 1,000 times to obtain the mean of the effect evaluation indicators and the 95% CI estimated by Monte Carlo method. The ranges of the calibrated parameters are shown in Table S12. The model calculation was realized through R 4.3.2.

In addition, during the simulation of population-based model, since the short-term implementation of intervention strategy may not result in qualitative change, and the overall quality of life among females tends to be negative within 10 years[18], the duration of effect evaluation was set at 20 years. Furthermore, assuming that the ongoing strategies were maintained, we calculated the annual vaccinating rate and cervical screening participation rate required to achieve the global goal of accelerating cervical cancer elimination (90% HPV vaccination coverage, 70% screening coverage, and 90% cervical cancer treatment coverage) by 2030 based on the current level of vaccine and screening coverages. This was assumed as the target strategy whose health and health economics benefits were also evaluated. After calculation, the overall annual vaccinating rate of the target strategy is 23.25%, and the ratio of different vaccine types was set according to the current ratio. The participation rate of cervical screening is 1.22 times higher than before, and the treatment rates of LSIL, HSIL, and CC are increased to 90% on this basis.

Table S12. The ranges of calibrated parameters

Parameters	Ranges	
	Lower bound	Upper bound
ξ_{cc1}	0.90103	0.99901
ξ_{cc2}	0.80079	0.89958
ξ_{cc3}	0.70035	0.79966
ξ_{cc4}	0.60018	0.69817
β	0.56720	0.57188
α	0.01506	0.02665
Infection duration	1.25590	1.51610
β_{if}	0.02791	0.06607
γ_{cin1}	0.47481	0.55450

β_{cin1}	0.16171	0.28698
γ_{cin2}	0.19954	0.29867
β_{cin2}	0.26362	0.43387
γ_{cin3}	0.01013	0.01676
β_{cin3}	0.04669	0.28703
β_{acc1}	0.33039	0.54700
β_{acc2}	0.40245	0.66872
β_{acc3}	0.51644	0.85195
s_1	0.11000	0.18989
s_2	0.17515	0.28992
s_3	0.46321	0.74747
s_4	0.68270	0.99755
ωd_{acc1}	0.01213	0.03564
ωs_{acc1}	0.82057	0.93839
ωd_{acc2}	0.02509	0.06383
ωs_{acc2}	0.68181	0.87973
ωd_{acc3}	0.06548	0.19057
ωs_{acc3}	0.07170	0.67694
ωd_{acc4}	0.19125	0.44885
ωs_{acc4}	0.00026	0.04755
κ_1	0.79133	0.99875
κ_2	0.53124	0.87904
κ_3	0.78038	0.83764
κ_4	0.90134	0.98938
Screening interval	3.00710	4.98690
Efficacy of cryotherapy to CIN	0.74343	0.91922
Efficacy of TA to CIN1	0.81409	0.95954
Efficacy of TA to CIN2/3	0.62234	0.86949
Efficacy of CKC	0.87017	0.91963
Efficacy of LEEP	0.85239	0.98996
α_m	0.01521	0.02697
γ_{im}（HPV-16）	0.28594	0.47446
γ_{im}（HPV-18）	0.54286	0.89872
γ_{im}（other hr-genotype）	0.51898	0.85750
β_{im}	0.03626	0.05991
γ_{lin}	0.04024	0.06644
β_{lin}	0.00392	0.00650
γ_{hin}	0.04010	0.06618
β_{hin}	0.00006	0.00008
ωs_c	0.62930	0.75491
ωd_c	0.10788	0.31104

4.1. Model outputs

The primary outcomes of epidemic trend prediction include the number of current cases of hr-HPV infection, the number of current cases in various stages of CIN and cervical cancer, and the cumulative five-year survival and death due to cervical cancer. The changes in the prevalence in each model compartment were visualized and presented using curves smoothed by cubic spline method. The primary outcomes of health benefits evaluation include the prevented cumulative hr-HPV infections compared to baseline, the prevented cumulative CIN and cervical cancer cases compared to baseline, and the prevented number of deaths due to cervical cancer compared to baseline. The overall health benefit is evaluated by calculating the quality of life among female population. The primary outcomes of the health economics benefit evaluation are the increased cost of preventive strategies, the increased quality-adjusted life years (QALYs), and the incremental cost-utility ratio (ICUR) compared to baseline.

4.2. Sensitivity analysis

The sensitivity analyses conducted in this study are shown in Table S13.

Table S13. The summary of sensitivity analyses

Parameters	Adjustment
overall vaccinating rate	-50%~+50%
overall screening rate	-50%~+50%
overall treatment rate	-50%~+50%
rural vaccinating rate	to urban level
rural screening rate	to urban level
rural treatment rate	to urban level
vaccinating rate of 2v vaccine	+0%~+10%
vaccinating rate of 4v vaccine	+0%~+10%
vaccinating rate of 9v vaccine	+0%~+10%
age-stratified vaccinating rate	-50%,-25%,+25%,+50%
screening time interval	-50%,-25%,+25%,+50%
screening participation rate (35-44 years old)	-50%,-25%,+25%,+50%
screening targeted age	35-44 years old; backward to 15, 25; forward to 54, 64
cost of 2v/4v/9v vaccine	-25%~+25%
cost of HPV testing/TCT/pathology/service	-25%~+25%

cost of LSIL/HSIL/CC1/CC2-3/CC4 treatment/hysterectomy/treatment service	-25%~+25%
discount rate	-25%~+25%
efficacy of 2v/4v/9v vaccine	-5%~+5%
sensitivity of HPV testing/TCT to LSIL/HSIL/CC	-5%~+5%
efficacy of treatment to CIN1-3/CC1-4	-5%~+5%

4.3. Scenario analysis

The primary HPV vaccination and cervical screening scenarios included in this study are shown in Figure S9 and S10, respectively.

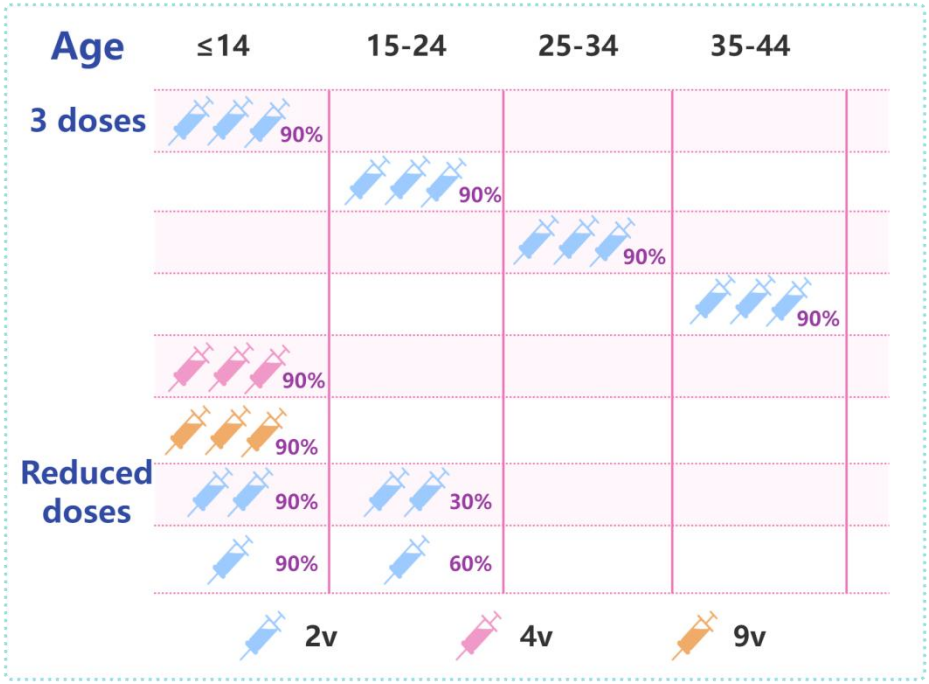

Figure S9. The primary HPV vaccination scenarios included in the study

Limited vaccine supply are considered. 3 doses vaccination targeted at different ages, or using different types of vaccine, 2 doses vaccination targeted at the early age and catch-up vaccination for those before 25, as well as single dose vaccination targeted at the early age and catch-up vaccination for those before 25 are the primary scenarios included in this study.

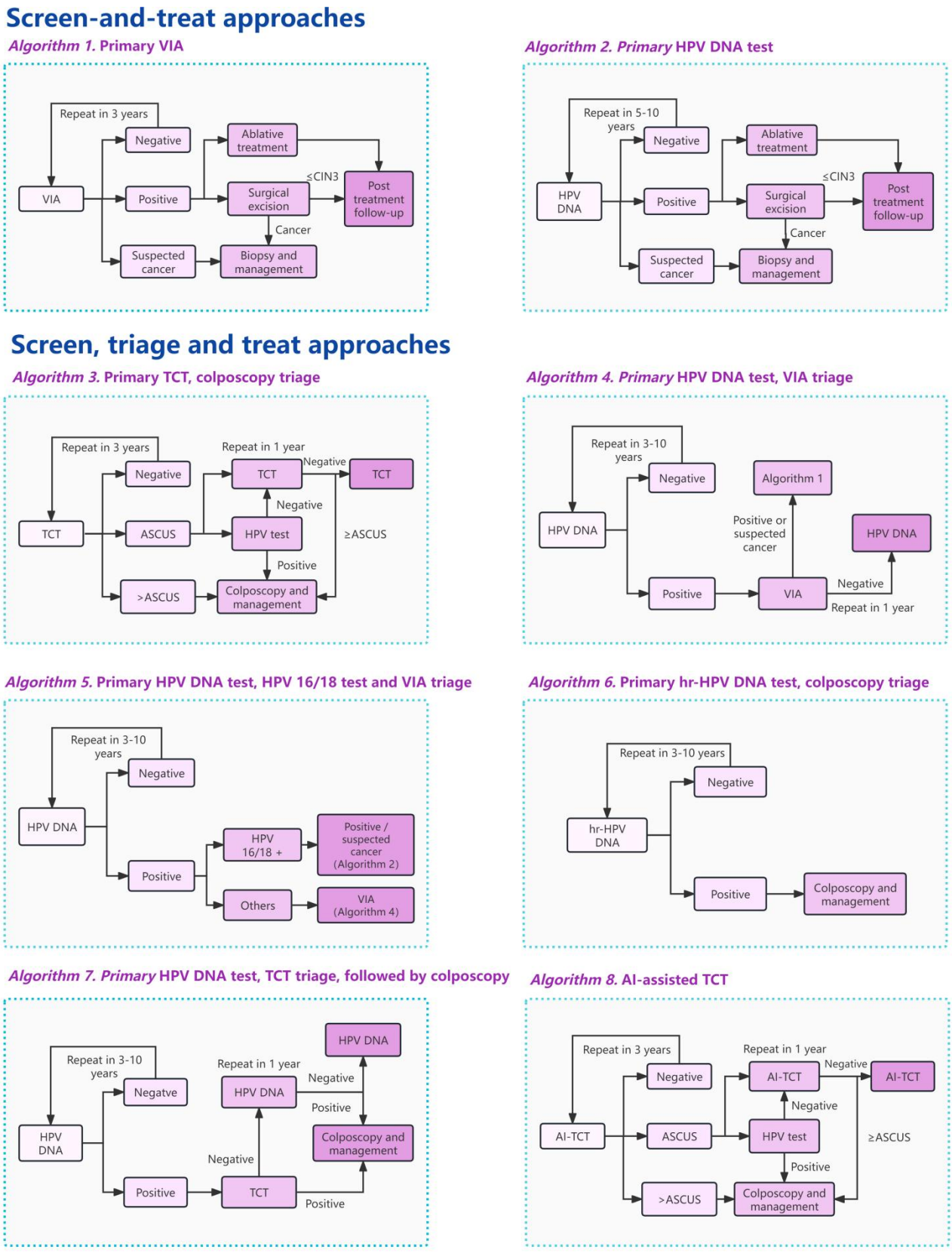

Figure S10. The primary cervical screening scenarios included in the study

Algorithm 1-7 are the screening pathways recommended by WHO. Algorithm 8 is the pathway using AI-TCT method based on Algorithm 3.

4.4. Health economics evaluation

In this study, the health economics benefits were evaluated by calculating the ICUR value, which was calculated by:

$$ICUR = {}^{\Delta Cost}/_{\Delta QALYs} \quad (4\text{-}1)$$

where ΔCost denotes the change in total cost, which was adjusted to the 2023 international USD dollar based on the annual discount rate (d), consumption index, and exchange rate. ΔQALYs represents the change in QALYs, which was calculated as the sum of the quality of life for among female population in each year, as follow:

$$QALYs = \sum_p QALYs_p = \sum_p \sum_t Quality_p(t) * I(t) \quad (4\text{-}2)$$

where $QALYs_p$ denotes the quality of life of individual p, $Quality(t)$ denotes the quality of life in the year t, $I(t)$ is the indicator function, indicating whether or not the individual survive.

The evaluation criteria for cost-utility analysis refer to the standard proposed by WHO. If the ICUR is less than the gross domestic product (GDP) per capita in China (13,013.18 USD in 2023), the intervention strategy is considered to have high cost-utility. If the ICUR value is 1-3 times the per capita GDP, the intervention strategy is considered to have cost-utility. If the ICUR value is higher than three times the per capita GDP, the intervention strategy is with no cost-utility. The costs of each intervention method and the quality of life of all the status are shown in Table S14 and S15.

Table S14. The parameters related to cost

Symbol	Implication	Value	Range	Source
Vaccination				
costv1	the price of bivalent vaccine (one dose)	49.54	48.98-55.98	[23,43]
costv2	the price of quadrivalent vaccine (one dose)	115.18	111.96-125.95	[23,43]
costv3	the price of ninvalent vaccine (one	185.15	181.94-202.92	[23,43]

	dose)			
costvs	vaccination service cost	3.83	2.87-4.79	[44]
Screening				
costVIA	the cost of VIA	2.55	1.93-3.16	[20]
costHPV	the cost of HPV testing	15.13	11.35-18.91	[23]
costLBC	the cost of LBC-based screening	9.64	7.23-12.05	[15]
costcol	the cost of colposcopy	6.01	1.73-10.28	[20]
costbio	the cost of biopsy	16.70	11.20-22.20	[20]
costss	screening service cost	25.6	20.64-30.56	[7]
Treatment				
costcryo	the cost of cryotherapy	4.5	1.7-7.4	[20]
costTA	the cost of thermal ablation	11.43	8.57-14.29	[45]
costCKC	the cost of CKC	1.5 times of LEEP	1.5 times of LEEP	[45]
costLEEP	the cost of LEEP	123.5	92.4-181.6	[20]
costhys	the cost of hysterectomy	315.6	151.3-479.8	[20]
$cost_{lsil}$	the treatment cost of LSIL	250.93	170.16-280.82	[18]
$cost_{hsil}$	the treatment cost of HSIL	2,146.1	2,100.51-2,191.68	[7]
$cost_{cins}$	service cost of CIN treatment	109.0	98.75-119.24	[7]
$cost_{cc1}$	the treatment cost of CC1	14,083.92	13,731.82-14,436.02	[46]
$cost_{cc23}$	the treatment cost of CC2/3	46,194.55	45,983.92-46,405.18	[7]
$cost_{cc4}$	the treatment cost of CC4	47,064.93	45,888.31-48,241.55	[46]
Other				

costhc1	the annual healthcare cost of CC1	633	316-949	[47]
costhc23	the annual healthcare cost of CC2/3	798	399-1197	[46]
costhc4	the annual healthcare cost of CC4	1056	528-1585	[46]
d	discount rate	0.03	0.00-0.08	[48]

NOTE: ALL the costs were adjusted according to Chinese consumer price indexes in the category of health, 2023 as the base year, and were adjusted to USD based on exchange rate.
VIA, visual inspection with acetic acid; LBC, liquid-based cytology.

Table S15. The utility scores (QALY) of each individual

Status	Value	Range	Source
S	1.000	/	assumed
I	0.996	0.991-1.000	[49]
Im	0.990	0.996-1.000	[18,49]
CIN1	0.938	0.73-1.00	[50]
CIN2/3	0.900	0.873-0.927	[51]
CIN treated	0.960	0.945-0.976	[18]
CC1	0.830	0.788-0.873	[51]
CC2	0.780	0.773-0.907	[51]
CC3	0.720	0.650-0.780	[51]
CC4	0.600	0.430-0.770	[51]
CC1 treated	0.705	0.490-0.810	[7]
CC2 treated	0.605	0.420-0.670	[7]
CC3 treated	0.560	0.420-0.700	[7]
CC4 treated	0.480	0.360-0.600	[7]
CCs	0.930	0.700-0.990	[16,20]
CCd	0.000	/	assumed

NOTE: QALY, quality-adjusted life year.

5. Results

Table S16 (a). The sample size of age-stratified cervical screening for each quarter during calibration in the training set

Age	Time												
	2020Q4	2021Q1	2021Q2	2021Q3	2021Q4	2022Q1	2022Q2	2022Q3	2022Q4	2023Q1	2023Q2	2023Q3	2023Q4
24-	116	116	82	128	46	28	81	69	47	53	37	36	62
25-34	3,859	2,859	3,166	2,754	2,868	708	1,012	1,086	1,829	2,069	2,052	1,527	1,366
35-44	3,332	2,500	3,148	2,013	3,215	1,656	2,905	2,562	1,755	1,946	2,389	1,890	1,274
45-54	1,163	795	1,017	675	1,135	200	360	596	565	647	850	711	452
55-64	332	239	316	231	275	53	81	102	207	290	342	303	169
65+	13	7	10	14	5	11	11	7	10	4	3	4	21

Table S16 (b). The sample size of age-stratified cervical screening for each quarter during calibration in the testing set

Age	Time												
	2020Q4	2021Q1	2021Q2	2021Q3	2021Q4	2022Q1	2022Q2	2022Q3	2022Q4	2023Q1	2023Q2	2023Q3	2023Q4
24-	69	51	51	59	37	26	42	61	18	17	30	24	36
25-34	2,429	1,808	2,040	1,751	1,799	417	631	617	1,118	1,371	1,310	940	822
35-44	2,146	1,597	2,082	1,255	2,075	989	1,801	1,590	1,128	1,216	1,573	1,161	752
45-54	767	467	624	419	735	145	224	338	366	424	539	448	294
55-64	178	142	214	156	171	28	49	67	114	178	213	173	83
65+	6	8	7	10	11	5	2	6	4	4	1	7	5

Table S17 (a). The sample size of cervical screening stratified by genotype in each quarter during calibration in the training set

Genotype	Time												
	2020Q4	2021Q1	2021Q2	2021Q3	2021Q4	2022Q1	2022Q2	2022Q3	2022Q4	2023Q1	2023Q2	2023Q3	2023Q4
16	172	89	121	90	103	50	56	81	57	44	64	66	29
18	62	30	62	48	29	18	32	27	19	31	48	23	38
31	26	23	17	33	15	13	16	14	15	7	18	30	5
33	47	28	40	25	22	11	16	32	29	26	28	41	26
45	17	19	6	17	17	8	3	14	10	0	13	8	12
52	318	241	331	243	274	116	209	143	153	175	231	162	144
58	140	119	172	111	130	42	64	65	84	55	114	79	58

Table S17 (b). The sample size of cervical screening stratified by genotype in each quarter during calibration in the testing set

Genotype	Time												
	2020Q4	2021Q1	2021Q2	2021Q3	2021Q4	2022Q1	2022Q2	2022Q3	2022Q4	2023Q1	2023Q2	2023Q3	2023Q4
16	104	65	78	80	73	26	27	29	38	41	51	31	36
18	28	25	27	26	34	8	22	24	19	11	28	17	17
31	20	23	22	17	18	13	12	5	5	8	18	5	11
33	54	17	27	19	23	8	12	14	17	14	15	19	13
45	14	0	5	0	5	5	5	7	0	8	3	2	0
52	225	166	213	141	202	80	108	115	88	80	173	116	83
58	104	82	84	71	73	26	47	43	45	58	81	51	32

Table S18. The sample size for cervical screening and prevalence of hr-HPV in each quarter of the real-world training and testing sets

Index	Time						
	2020Q3	2020Q4	2021Q1	2021Q2	2021Q3	2021Q4	2022Q1
Sample size in training set	11,085	8,815	6,515	7,739	5,851	7,544	2,656
Prevalence in training set	0.1287	0.1554	0.1524	0.1685	0.1720	0.1414	0.1693
Sample size in testing set	6,724	5,595	4,073	5,018	3,650	4,828	1,610
Prevalence in testing set	0.1288	0.1633	0.1526	0.1532	0.1717	0.1487	0.1716

Continued Table S18

Index	Time						
	2022Q2	2022Q3	2022Q4	2023Q1	2023Q2	2023Q3	2023Q4
Sample size in training set	4,450	4,422	4,413	5,009	5,673	4,471	3,344
Prevalence in training set	0.1637	0.1450	0.1484	0.1219	0.1564	0.1628	0.1803
Sample size in testing set	2,749	2,679	2,748	3,210	3,666	2,753	1,992
Prevalence in testing set	0.1675	0.1580	0.1286	0.1217	0.1533	0.1709	0.1703

Table S19. The point estimation of hr-HPV prevalence under the optimal parameter combination and the top 1% parameter combination bootstrap samples after calibration based on the ODE model

Type	Time						
	2020Q4	2021Q1	2021Q2	2021Q3	2021Q4	2022Q1	2022Q2
The optimal parameter combination	0.1407	0.1526	0.1612	0.1654	0.1654	0.1620	0.1561
The bootstrap sample of top 1% parameters	0.1406	0.1524	0.1610	0.1653	0.1656	0.1627	0.1572

Continued Table S19

Type	Time					
	2022Q3	2022Q4	2023Q1	2023Q2	2023Q3	2023Q4
The optimal parameter combination	0.1483	0.1395	0.1301	0.1426	0.1663	0.1826
The bootstrap sample of top 1% parameters	0.1500	0.1417	0.1298	0.1476	0.1704	0.1862

Table S20. The prevalence of females in each model compartment among the total population under ongoing strategies

Status	Simulation period										
	2023	2024	2025	2026	2027	2028	2029	2030	2031	2032	2033
SIRS											
S	0.5022	0.3898	0.3504	0.3377	0.3353	0.3372	0.3408	0.3452	0.3498	0.3543	0.3585
I	0.1930	0.1973	0.1415	0.0932	0.0612	0.0413	0.0292	0.0217	0.0171	0.0143	0.0125
Im	0.4076	0.5162	0.5951	0.6402	0.6619	0.6694	0.6684	0.6624	0.6534	0.6426	0.6309
CIN ($\times 10^{-2}$)											
CIN	1.5924	1.4932	1.4505	1.3041	1.1111	0.9205	0.7539	0.6164	0.5065	0.4203	0.3532
CIN1	1.1398	1.0296	0.9509	0.7847	0.6021	0.4461	0.3271	0.2415	0.1818	0.1411	0.1136
CIN2	0.3394	0.3042	0.2991	0.2842	0.2516	0.2097	0.1677	0.1310	0.1012	0.0784	0.0615
CIN3	0.1131	0.1594	0.2004	0.2351	0.2574	0.2648	0.2590	0.2440	0.2235	0.2008	0.1780
CC ($\times 10^{-3}$)											
CC	1.8417	1.5271	1.3626	1.2960	1.2842	1.2910	1.2907	1.2701	1.2255	1.1595	1.0778
CC1	0.7404	0.5158	0.4663	0.4887	0.5326	0.5700	0.5874	0.5820	0.5571	0.5182	0.4713
CC2	0.5555	0.4203	0.3256	0.2783	0.2625	0.2618	0.2645	0.2636	0.2565	0.2432	0.2251
CC3	0.3703	0.3347	0.2750	0.2247	0.1913	0.1722	0.1622	0.1563	0.1510	0.1446	0.1363
CC4	0.1852	0.2661	0.3055	0.3140	0.3076	0.2967	0.2864	0.2779	0.2706	0.2632	0.2548
Removed ($\times 10^{-3}$)											
Rd	0.0000	0.0858	0.1668	0.2407	0.3096	0.3758	0.4407	0.5044	0.5665	0.6262	0.6828
Rs	0.0000	0.2332	0.4203	0.5868	0.7475	0.9091	1.0720	1.2330	1.3880	1.5328	1.6644

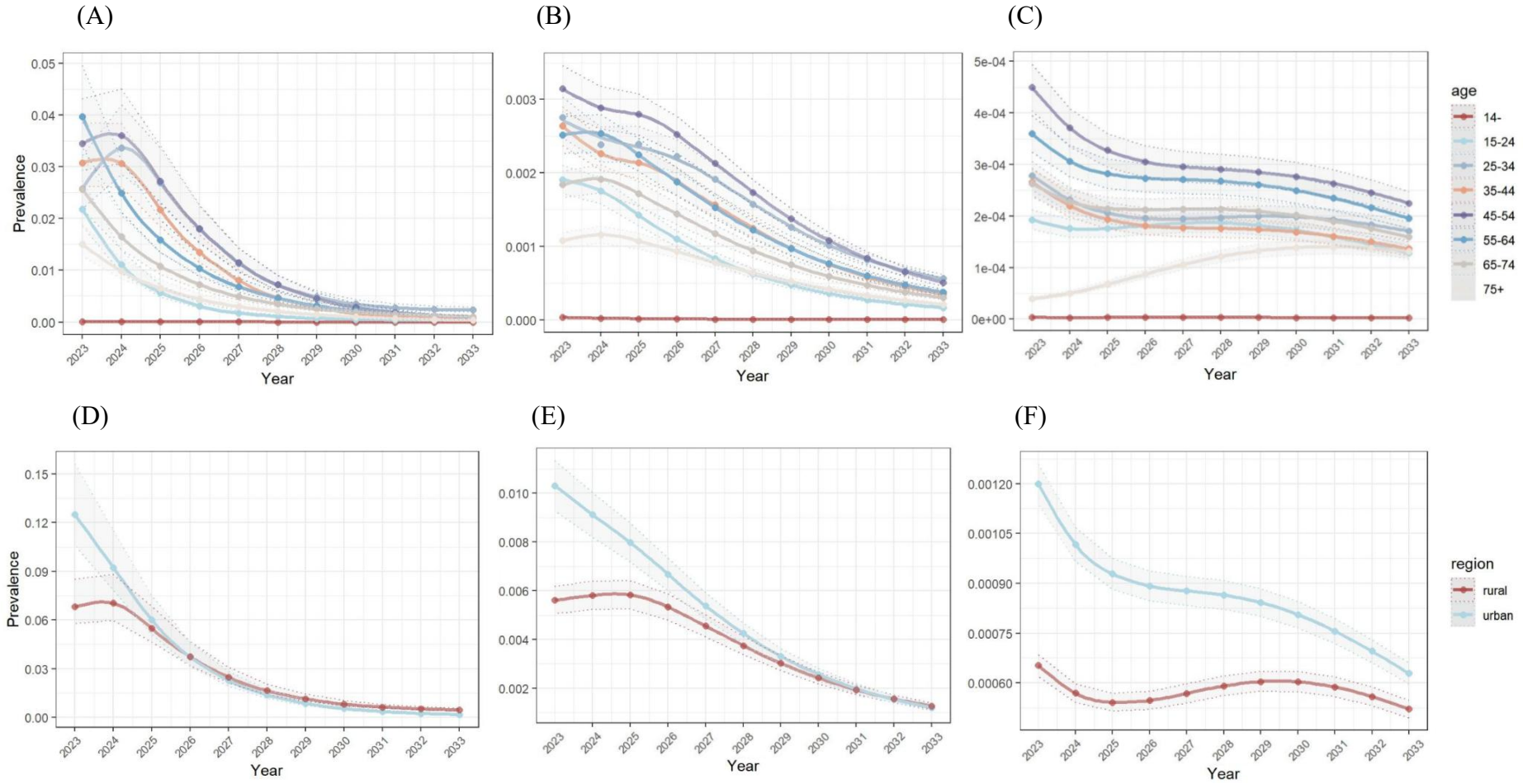

Figure S11. The stratified trends of different status among the total female population under ongoing strategies. (A)-(C): The age-stratified trend of hr-HPV infections, CIN and CC. (D)-(E): The urban- and rural-stratified trend of hr-HPV infections, CIN and CC. *x-axis is the simulation year, y-axis is the prevalence in each status.*

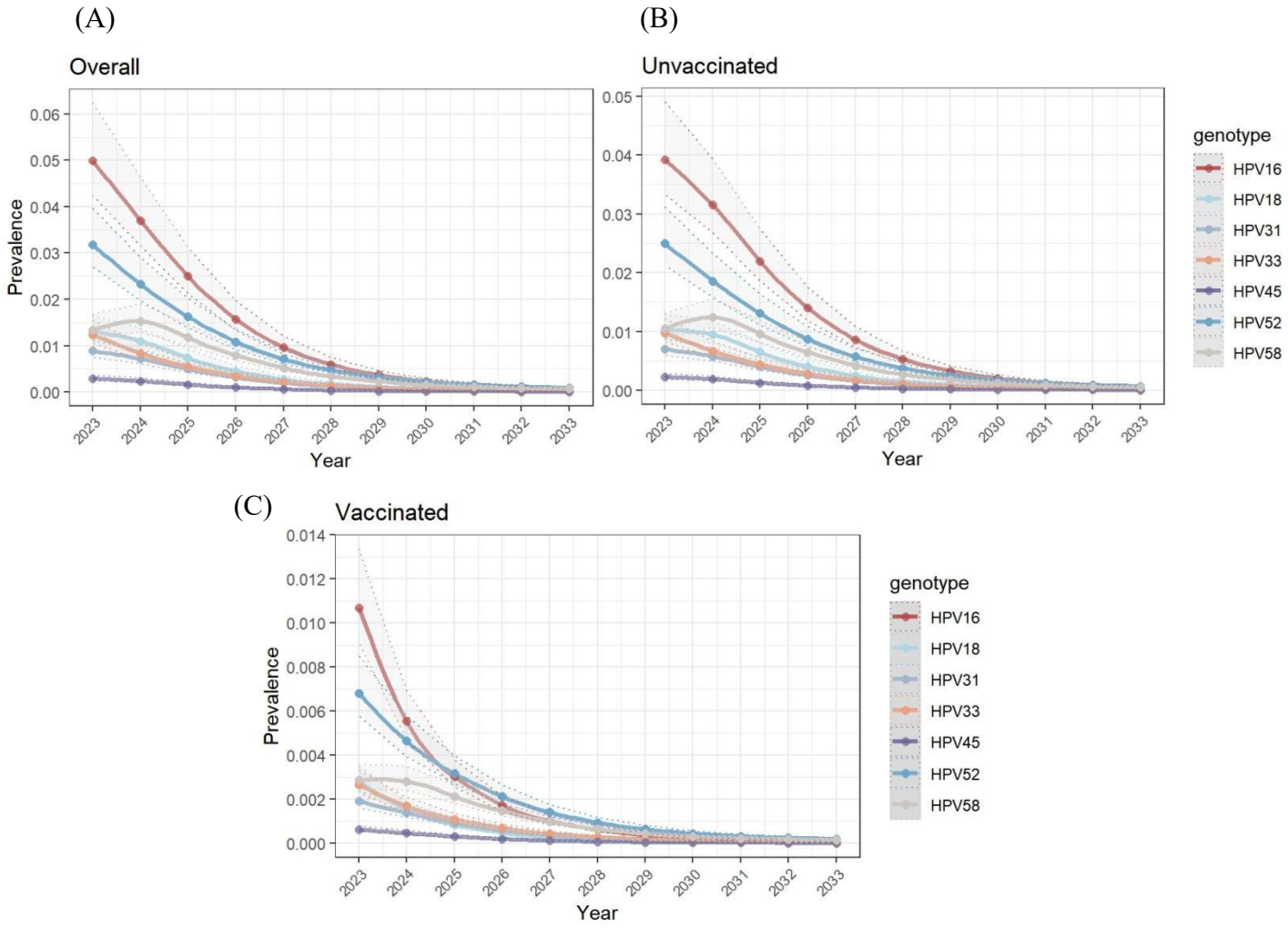

Figure S12. The genotype-specific trend of hr-HPV infections under ongoing strategies. (A) The overall female population. (B) The unvaccinated group. (C) The vaccinated group.

x-axis is the simulation year, y-axis is the hr-HPV prevalences.

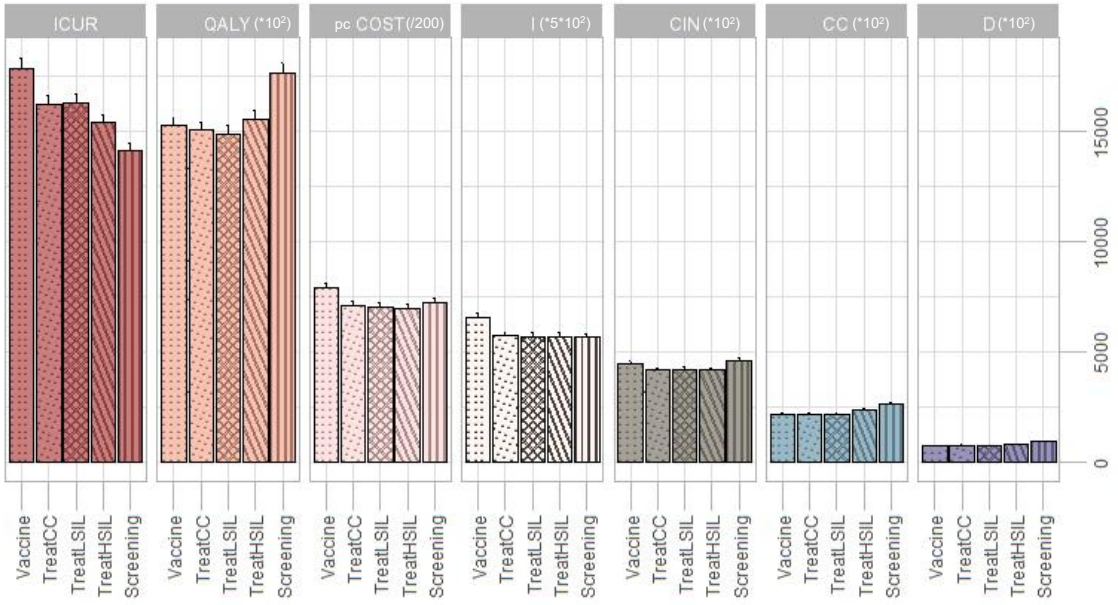

Figure S13. The sensitivity analysis result of improving the rural intervention participation rate to the urban level.

(A)

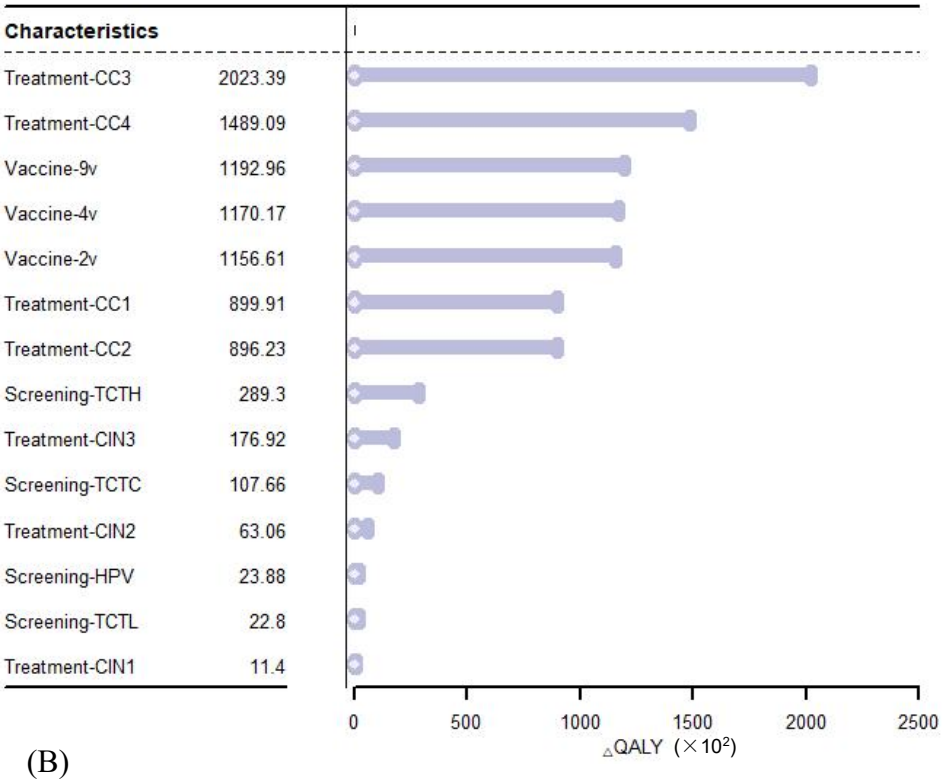

(B)

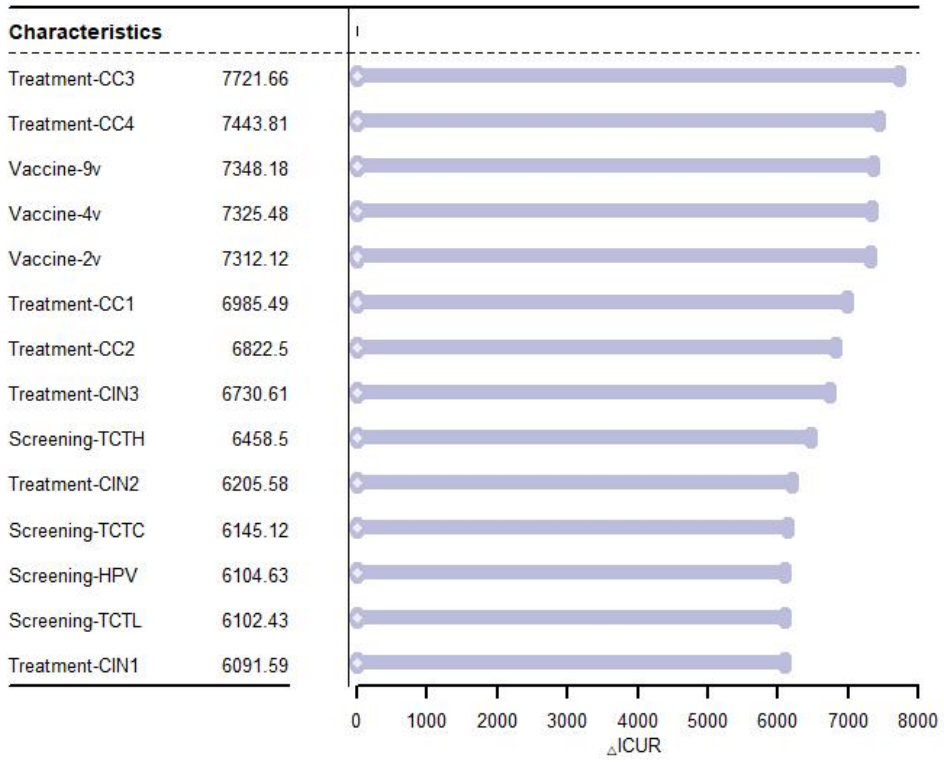

Figure S14. Changes in QALYs and ICUR caused by fluctuations of 5% in vaccine efficacy, treatment efficacy, and screening sensitivity under ongoing strategies. (A) QALYs; (B) ICUR. *Vaccine-2v/4v/9v denotes vaccination with 2v/4v/9v vaccines. Screening-HPV denotes HPV testing; screening-TCTL/TCTH/TCTC denotes TCT towards LSIL/HSIL/CC. Treatment-CIN1-3 denotes the treatment to CIN stage 1-3; treatment-CC1-4 denotes the treatment to CC stage 1-4.*

(A)

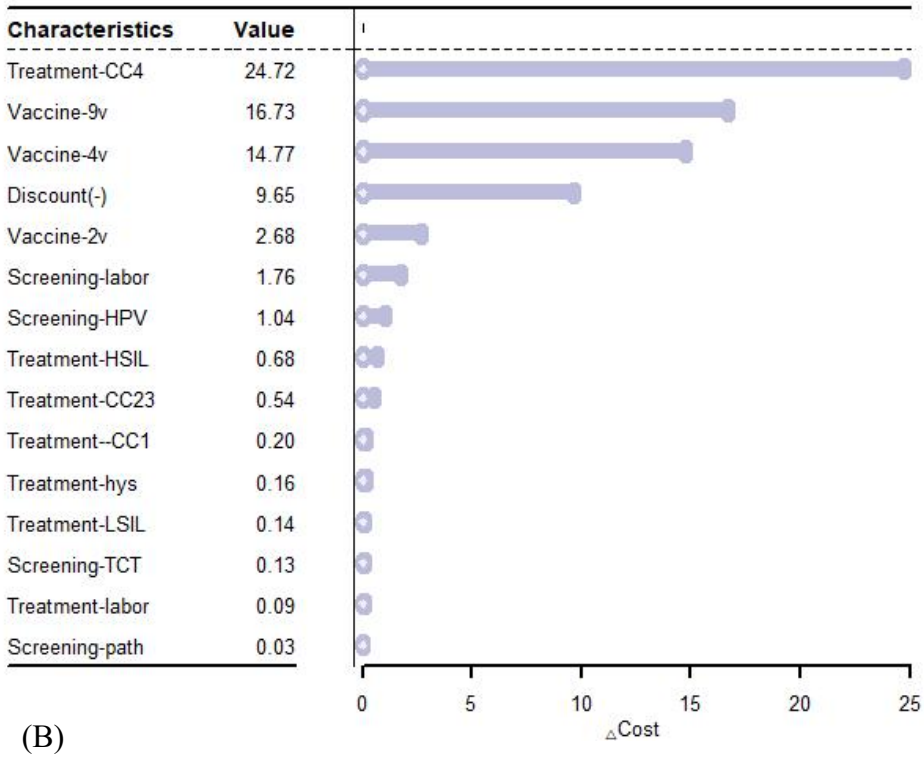

(B)

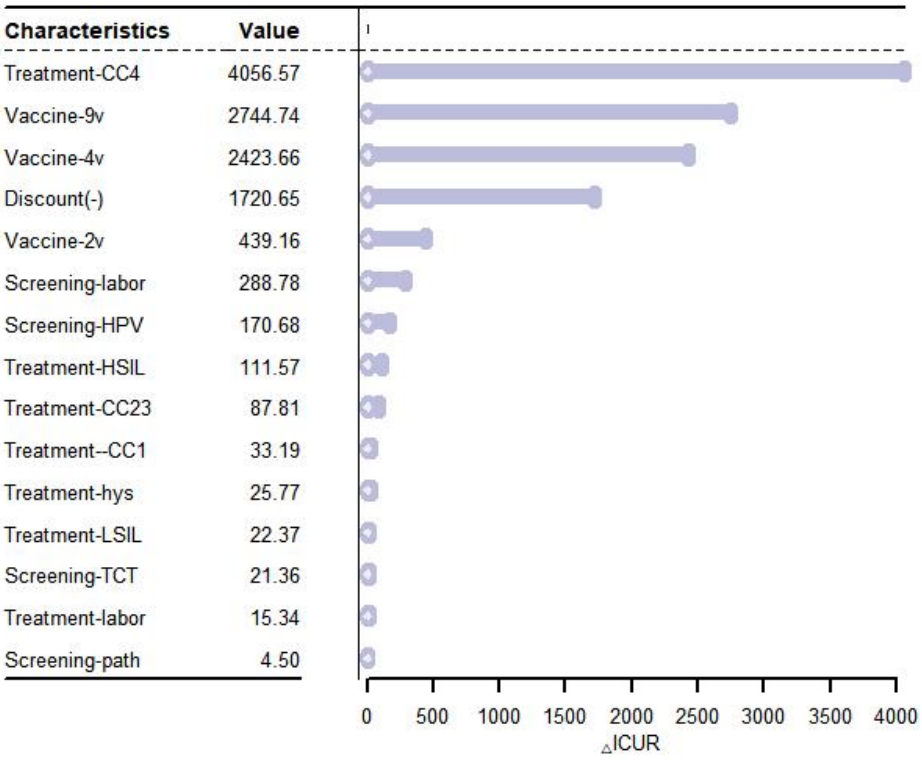

Figure S15. Changes in per capita cost and ICUR caused by fluctuations of 25% in vaccine, treatment and screening cost under ongoing strategies. (A) pc Cost; (B) ICUR.

Discount(-), the discount rate(×-1); labor, the service cost; hys, hysterectomy; path, pathology.

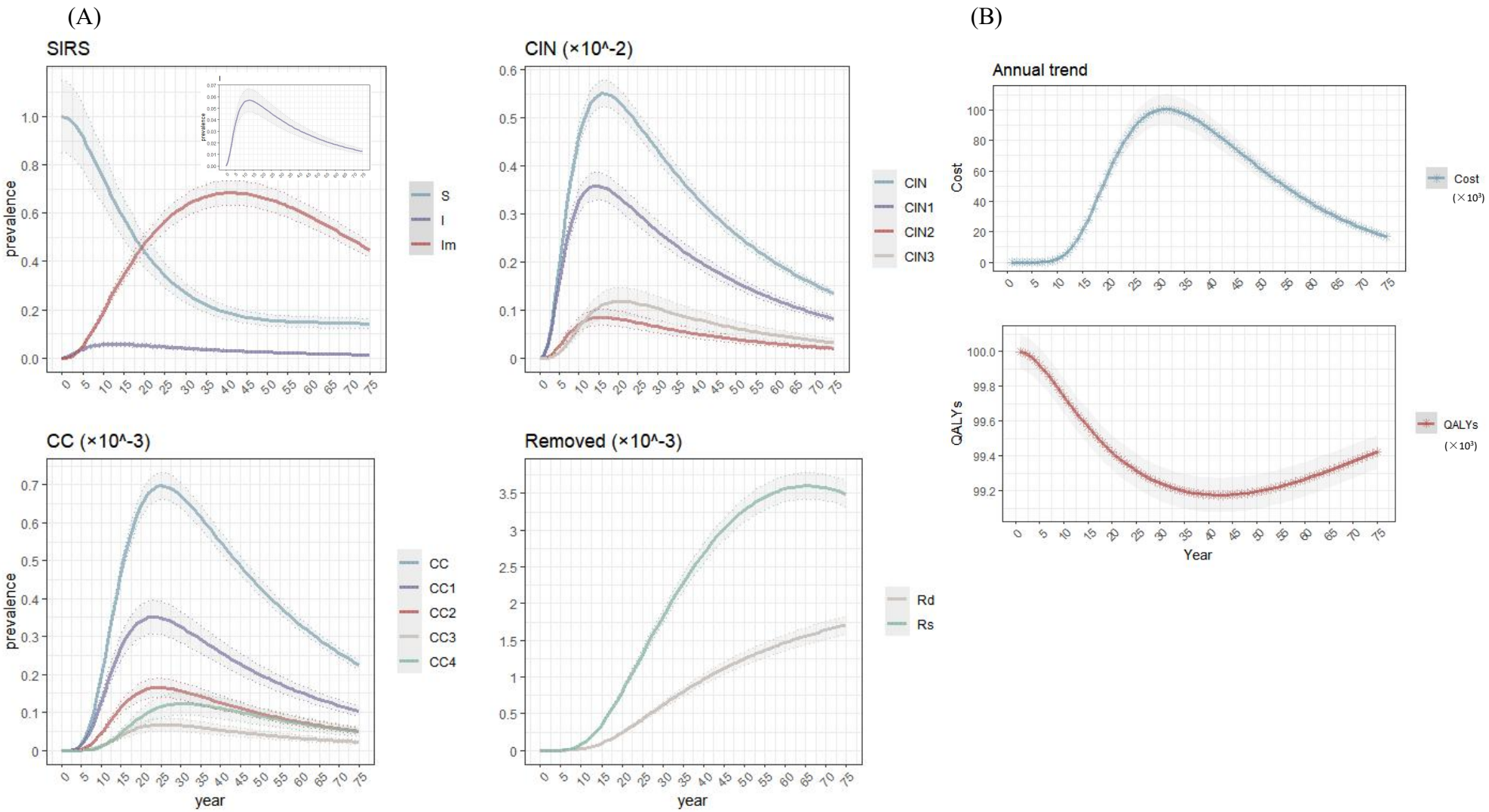

Figure S16. The trends of health and health economics indicators under the BASELINE among 100,000 women under the age of 14 within 75 years. (A) The trends of hr-HPV infections and cervical cancers at various stages. (B) The annual cost and overall QALYs.

x-axis is the simulation year. y-axis is the prevalence (A) and value (B).

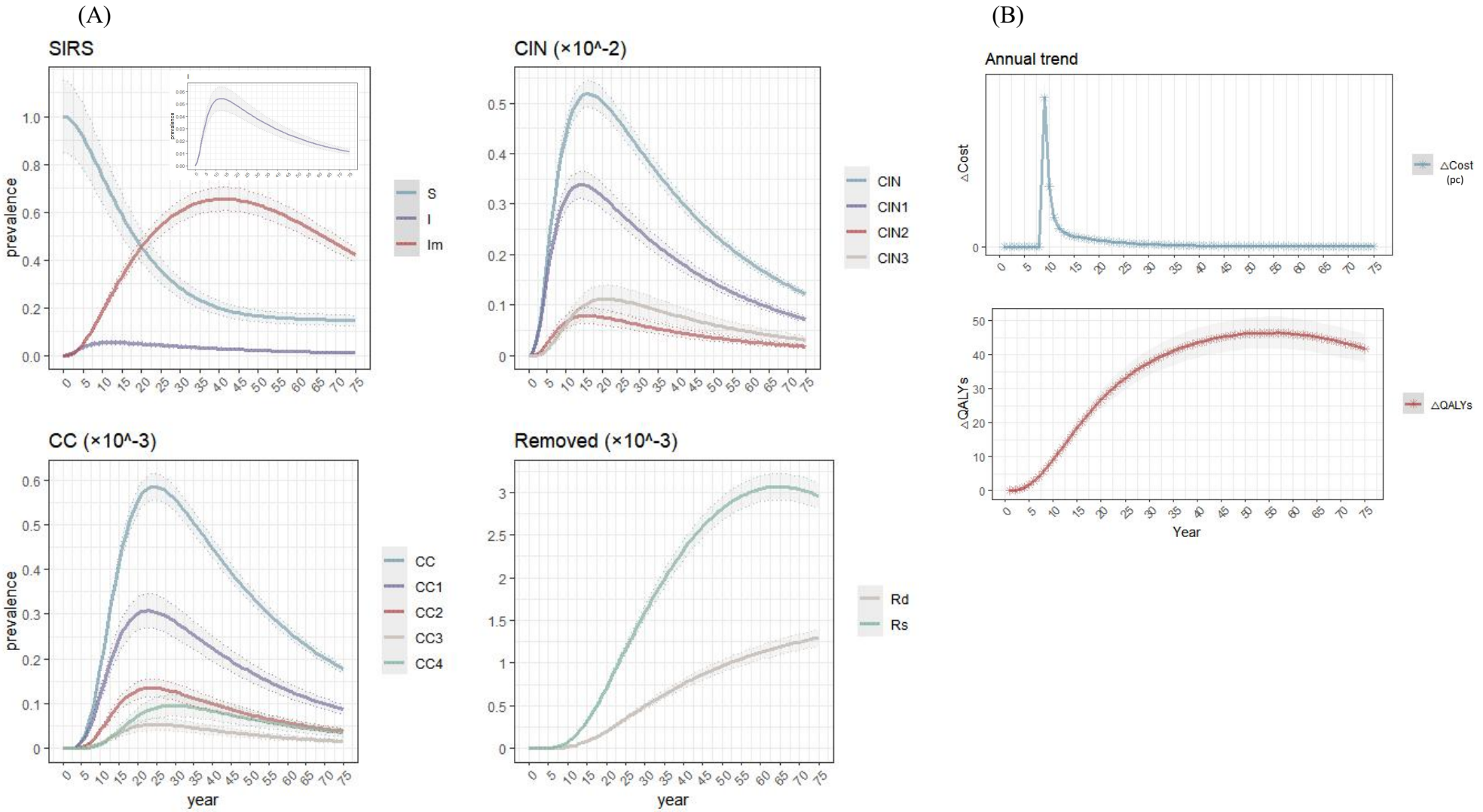

Figure S17. The trends of health and health economics indicators under the ONGOING strategies among 100,000 women under the age of 14 within 75 years. (A) The trends of hr-HPV infections and cervical cancers at various stages. (B) The annual cost and overall QALYs. *x-axis is the simulation year. y-axis is the prevalence (A) and value (B).*

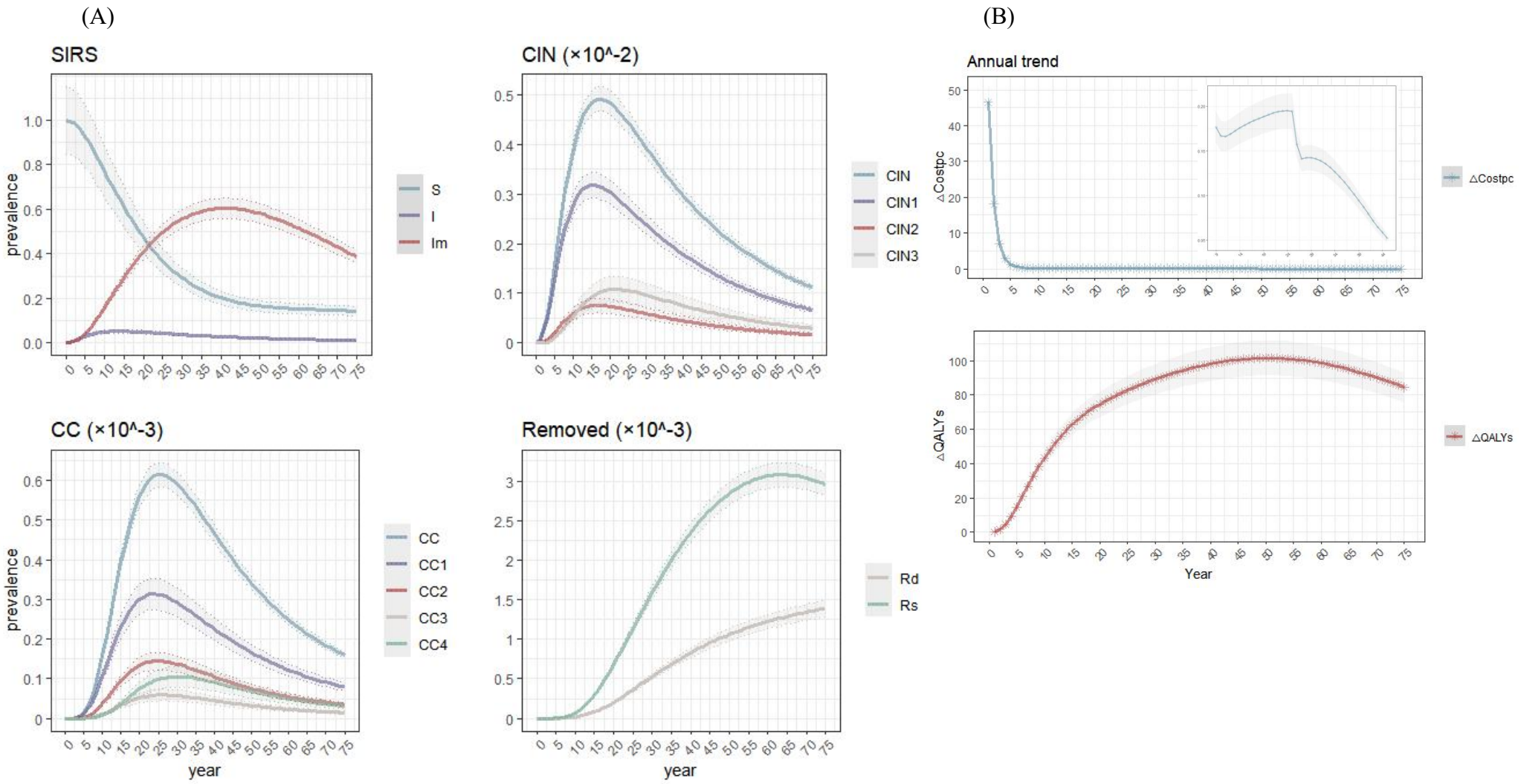

Figure S18. The trends of health and health economics indicators under the OPTIMAL strategies among 100,000 women under the age of 14 within 75 years. (A) The trends of hr-HPV infections and cervical cancers at various stages. (B) The annual cost and overall QALYs. *x-axis is the simulation year. y-axis is the prevalence (A) and value (B).*

6. References

[1] LI K, LI Q, SONG L , *et al.* The distribution and prevalence of human papillomavirus in women in mainland China. Cancer, 2019, 125(7): 1030-1037.

[2] WANG H, ZHAO J, LIU X , *et al.* The Prevalence and Genotype Distribution of Human Papillomaviruses Among Men in Henan Province of China. Frontiers in medicine, 2021, 8: 676401.

[3] ZHAO M, LIU H, CHEN X , *et al.* Sexual network and condom use among male migrants in the context of China's gender imbalance. AIDS Care, 2022, 34(8): 1048-1052.

[4] DE VRIES A, DEN DAAS C, WILLEMSTEIN I J M , *et al.* Interventions Promoting Condom Use Among Youth: A Systematic Review. J Adolesc Health, 2024, 74(4): 644-656.

[5] BARNABAS R V, LAUKKANEN P, KOSKELA P , *et al.* Epidemiology of HPV 16 and cervical cancer in Finland and the potential impact of vaccination: mathematical modelling analyses. PLoS medicine, 2006, 3(5): e138.

[6] KONG F P A O H. http://www.famplan.org.hk, 2023.

[7] CHOI H C W, LEUNG K, CHAN K K L , *et al.* Maximizing the cost-effectiveness of cervical screening in the context of routine HPV vaccination by optimizing screening strategies with respect to vaccine uptake: a modeling analysis. BMC medicine, 2023, 21(1): 48.

[8] GASKINS A J, SUNDARAM R, BUCK LOUIS G M , *et al.* Predictors of Sexual Intercourse Frequency Among Couples Trying to Conceive. J Sex Med, 2018, 15(4): 519-528.

[9] LI Y, LIU S, YAO J , *et al.* Influence Factors of Sexual Intercourse Frequency in Infertile Couples without Sexual Dysfunction in Southwest China: A Retrospective Study. Urol Int, 2021, 105(11-12): 949-955.

[10] WANG B, PENG X, LIANG B , *et al.* Sexual activity, sexual satisfaction and their correlates among older adults in China: findings from the sexual well-being (SWELL) study. The Lancet regional health. Western Pacific, 2023, 39: 100825.

[11] PENG J, PENG E. Factors influencing intercourse frequency among the young and middle-aged men. Zhong Nan Da Xue Xue Bao Yi Xue Ban, 2022, 47(9): 1260-1266.

[12] STATISTICS N B O. Statistical Yearbook. https://www.stats.gov.cn/sj/ndsj/, 2023.

[13] STATISTICS S M B O. Shenzhen Population Census. http://tjj.sz.gov.cn/, 2023.

[14] JOHNSON H C, ELFSTRöM K M, EDMUNDS W J. Inference of type-specific HPV transmissibility, progression and clearance rates: a mathematical modelling approach. PloS one, 2012, 7(11): e49614.

[15] XIA C, HU S, XU X , *et al.* Projections up to 2100 and a budget optimisation strategy towards cervical cancer elimination in China: a modelling study. The Lancet. Public health, 2019, 4(9): e462-e472.

[16] LIU Y J, ZHANG Q, HU S Y , *et al.* Effect of vaccination age on cost-effectiveness of human papillomavirus vaccination against cervical cancer in China. BMC Cancer, 2016, 16: 164.

[17] HAEUSSLER K, DEN HOUT A V, BAIO G. A dynamic Bayesian Markov model for health economic evaluations of interventions in infectious disease. BMC Med Res Methodol, 2018, 18(1): 82.

[18] XIA C, XU X, ZHAO X , *et al.* Effectiveness and cost-effectiveness of eliminating cervical cancer through a tailored optimal pathway: a modeling study. BMC medicine, 2021, 19(1): 62.

[19] SAWAYA G F, SANSTEAD E, ALARID-ESCUDERO F , *et al.* Estimated Quality of Life and Economic Outcomes Associated With 12 Cervical Cancer Screening Strategies: A Cost-effectiveness Analysis. JAMA Intern Med, 2019, 179(7): 867-878.

[20] ZOU Z, FAIRLEY C K, ONG J J , *et al.* Domestic HPV vaccine price and economic returns for cervical cancer prevention in China: a cost-effectiveness analysis. The Lancet. Global health, 2020, 8(10): e1335-e1344.

[21] LU H, LI L, CHENG Y , *et al.* Timely Estimates of 5-Year Relative Survival for Patients With Cervical Cancer: A Period Analysis Using Cancer Registry Data From Taizhou, Eastern China. Frontiers in public health, 2022, 10: 926058.

[22] CHESSON H W, MEITES E, EKWUEME D U , *et al.* Cost-effectiveness of nonavalent HPV vaccination among males aged 22 through 26 years in the United States. Vaccine, 2018, 36(29): 4362-4368.

[23] LI Y, LIN Y F, WU X , *et al.* Effectiveness and cost-effectiveness of human papillomavirus vaccination strategies among men who have sex with men in China: a modeling study. Front Immunol, 2023, 14: 1197191.

[24] LIN A, ONG K J, HOBBELEN P , *et al.* Impact and Cost-effectiveness of Selective Human Papillomavirus Vaccination of Men Who Have Sex With Men. Clinical infectious diseases : an official publication of the Infectious Diseases Society of America, 2017, 64(5): 580-588.

[25] GIULIANO A R, PALEFSKY J M, GOLDSTONE S , *et al.* Efficacy of quadrivalent HPV vaccine against HPV Infection and disease in males. The New England journal of medicine, 2011, 364(5): 401-411.

[26] KANG L N, CASTLE P E, ZHAO F H , *et al.* A prospective study of age trends of high-risk human papillomavirus infection in rural China. BMC Infect Dis, 2014, 14: 96.

[27] LI M, LIU T, LUO G , *et al.* Incidence, persistence and clearance of cervical human papillomavirus among women in Guangdong, China 2007-2018: A retrospective cohort study. Journal of infection and public health, 2021, 14(1): 42-49.

[28] YIN X, ZHANG M, WANG F , *et al.* A national cross-sectional study on the influencing factors of low HPV vaccination coverage in mainland China. Frontiers in public health, 2022, 10: 1064802.

[29] SONG Y F, LIU X X, YIN Z D. Estimated vaccination rate of human papillomavirus vaccine for women aged 9-45 in China from 2018 to 2020. Chinese Vaccines and Immunization, 2021, 27(5): 570-575.

[30] QIAO Y L, WU T, LI R C , *et al.* Efficacy, Safety, and Immunogenicity of an Escherichia coli-Produced Bivalent Human Papillomavirus Vaccine: An Interim Analysis of a Randomized Clinical Trial. Journal of the National Cancer Institute, 2020, 112(2): 145-153.

[31] JOURA E A, GIULIANO A R, IVERSEN O E , *et al.* A 9-valent HPV vaccine against infection and intraepithelial neoplasia in women. The New England journal of medicine, 2015, 372(8): 711-723.

[32] ZHANG J, ZOU B Y, XIAO Q. Analysis of cervical cancer screening status in a large tertiary hospital from 2008 to 2017. Sichuan Medical Journal, 2019, 40(5): 445-448.

[33] MU H J, YU L Y, LI Y X. Analysis of Breast Cancer and Cervical Cancer Screening Status and Influencing Factors among Female Residents in Urban and Rural Areas of Liaoning Province. Chinese Public Health Management, 2015, 31(2): 197-198+201.

[34] WANG S M, YAN H J, REN W H. Progress in cervical cancer prevention and control in China. Chinese Journal of Preventive Medicine, 2023, 24(12): 1366-1370.

[35] ZONG L J, ZHANG Y Z, YANG X S , *et al.* Evaluation of several screening approaches for detection of cervical lesions in rural Shandong, China. Asian Pac J Cancer Prev, 2015, 16(5): 1907-1912.

[36] CHENG J Y, BIAN M L, MA L , *et al.* Evaluation of the effectiveness of testing for 14 high-risk HPV types (16 and 18) in cervical cancer screening. http://www.cogonline.com/info/132067934143932347_1, 2014.

[37] PAN Q J, HU S Y, ZHANG X , *et al.* Pooled analysis of the performance of liquid-based cytology in population-based cervical cancer screening studies in China. Cancer Cytopathol, 2013, 121(9): 473-482.

[38] DOLMAN L, SAUVAGET C, MUWONGE R , *et al.* Meta-analysis of the efficacy of cold coagulation as a treatment method for cervical intraepithelial neoplasia: a systematic review. Bjog, 2014, 121(8): 929-942.

[39] ZHAO X L, LIU Z H, ZHAO S , *et al.* Efficacy of point-of-care thermal ablation among high-risk human papillomavirus positive women in China. International journal of cancer, 2021, 148(6): 1419-1427.

[40] WANG L, LIU X, ZHANG J , *et al.* Evaluation of the efficacy and safety of 5-aminolevulinic acid-mediated

photodynamic therapy in women with high-risk HPV persistent infection after cervical conization. Photodiagnosis Photodyn Ther, 2022, 40: 103144.

[41] WU J, JIA Y, LUO M , *et al.* Analysis of Residual/Recurrent Disease and Its Risk Factors after Loop Electrosurgical Excision Procedure for High-Grade Cervical Intraepithelial Neoplasia. Gynecol Obstet Invest, 2016, 81(4): 296-301.

[42] LIU Y J, KEANE A, SIMMS K T , *et al.* Development and application of a framework to estimate health care costs in China: The cervical cancer example. PloS one, 2019, 14(10): e0222760.

[43] WUHAN.COM. Hpv Bivalent, Quadrivalent and Nine-valent Vaccines Price List. https://www.wuhan.com/life/80158.html, 2021.

[44] YU W, LU M, WANG H , *et al.* Routine immunization services costs and financing in China, 2015. Vaccine, 2018, 36(21): 3041-3047.

[45] ZHAO X L, ZHAO S, XIA C F , *et al.* Cost-effectiveness of the screen-and-treat strategies using HPV test linked to thermal ablation for cervical cancer prevention in China: a modeling study. BMC medicine, 2023, 21(1): 149.

[46] LIU N, MITTMANN N, COYTE P C , *et al.* Phase-specific healthcare costs of cervical cancer: estimates from a population-based study. Am J Obstet Gynecol, 2016, 214(5): 615.e611-615.e611.

[47] INSINGA R P, YE X, SINGHAL P K. Healthcare resource use and costs associated with cervical, vaginal and vulvar cancers in a large U.S. health plan. Gynecologic oncology, 2008, 111(2): 188-196.

[48] WALKER D G, HUTUBESSY R, BEUTELS P. WHO Guide for standardisation of economic evaluations of immunization programmes. Vaccine, 2010, 28(11): 2356-2359.

[49] BAINS I, CHOI Y H, SOLDAN K , *et al.* Clinical impact and cost-effectiveness of primary cytology versus human papillomavirus testing for cervical cancer screening in England. Int J Gynecol Cancer, 2019, 29(4): 669-675.

[50] VAN ROSMALEN J, DE KOK I M, VAN BALLEGOOIJEN M. Cost-effectiveness of cervical cancer screening: cytology versus human papillomavirus DNA testing. Bjog, 2012, 119(6): 699-709.

[51] ZHAO Z M, PAN X F, LV S H , *et al.* Quality of life in women with cervical precursor lesions and cancer: a prospective, 6-month, hospital-based study in China. Chin J Cancer, 2014, 33(7): 339-345.